Black Box Uncertainty Analysis for Semantic Segmentation

Anonymous authors
Paper under double-blind review

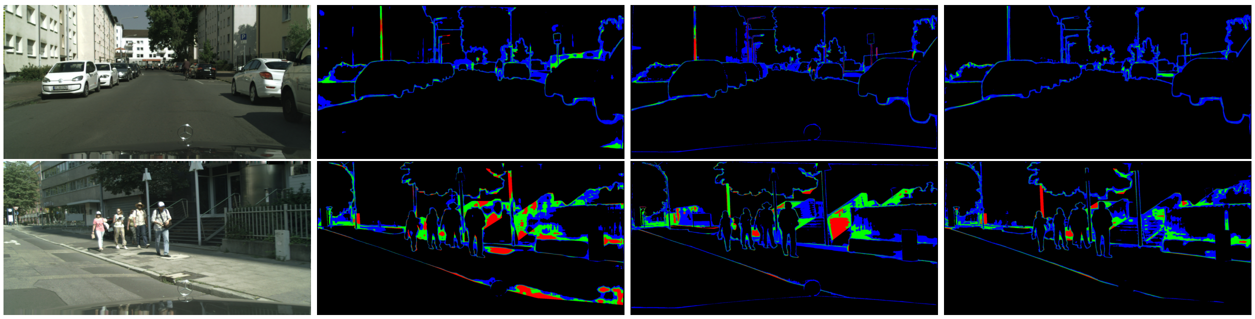

Figure 1: A couple of examples show how well the entropy of predicted outputs correlates with misclassified pixels. Green indicates misclassified pixels with high entropy, red shows misclassified pixels with low entropy, and blue shows correctly classified pixels with high entropy. Images in each row show the input and outputs from DRN D-22, OneFormer ConvNeXt-L and SegFormer B5, respectively. We note that entropy captures misclassified pixels with high recall.

Abstract

Semantic segmentation has become an important task in computer vision with the growth of self-driving cars, medical image segmentation, etc. Although current models provide excellent results, they are still far from perfect. While there has been significant work in trying to improve the performance, both with respect to accuracy and speed of segmentation, there has been little work which analyses the failure cases of such systems. In this work, we aim to provide an analysis of how segmentation fails across different models and consider the question of whether these can be predicted reasonably at test time. To do so, we explore existing uncertainty-based metrics and see how well they correlate with misclassifications, allowing us to define the degree of trust we put in the output of our prediction models. Through several experiments on three different models across three datasets, we show that simple measures such as entropy can be used to capture misclassification with high recall.

1 Introduction

Semantic segmentation is defined as a task which involves taking an image and labelling each pixel of the image as belonging to one of a set of predefined classes. With the advent of self-driving cars, path-finding robots, and various other such problems, semantic segmentation has become essential in the field of computer vision, as all of these applications rely on being able to segment, parse and understand the scene they see in order to take appropriate action. Semantic segmentation is even used in the medical field to segment areas of medical images for analysis. When used for such critical tasks, it is of utmost importance that the models we propose provide us with accurate results or some confidence metrics which can be used to rely on their outputs.

Most of the earlier approaches to semantic segmentation involve using Convolutional Neural Networks (CNN) to extract features and predict the segmentation class for each pixel. Examples of such approaches include Chen et al. (2014); Yu et al. (2017); Chen et al. (2017). Some of these approaches also utilise Conditional Random Fields (CRF) to improve their results further. More recent approaches use Transformer-based architectures such as Cheng et al. (2021); Xie et al. (2021); Jain et al. (2023b;a). Cheng et al. (2021) also utilises masked predictions for each class rather than simple pixel-wise multi-class predictions.

Although we now have a wealth of approaches that target semantic segmentation, the uncertainty quantification for their predictions is relatively less well-studied. This is especially true during test time since we cannot judge the model against ground truth predictions. For example, consider the case when there is a domain shift in the inputs during test time; how do we trust the output of our network without any form of confidence or trust metric?

There have been works which look at uncertainty in deep neural networks in general (Gawlikowski et al., 2023; Grathwohl et al., 2019; Hendrycks & Gimpel, 2016), including relatively new ones like Vazhentsev et al. (2022), which specifically considers uncertainty in Transformer networks. For semantic segmentation, we have works such as Xia et al. (2020); Rahman et al. (2022), which aim to detect failures and out-of-distribution samples. However, they use separate networks that require additional training. Our work explicitly focuses on obtaining such information at test time without any extra networks or training. By this, we mean that without any knowledge of the architecture, at test time, we wish to know whether our model has succeeded in semantic segmentation or not. Considering the gravity of this task, we believe that there should be a study of the same for the sake of understanding these networks better.

In this paper, we first look at where these segmentation networks fail to predict the correct classes (Section 3). We then ask questions such as, *"Knowing where these networks fail, can we predict these failures?"*, and *"How well do current approaches of gauging uncertainty correlate with misclassification?"*. To this end, we perform a series of experiments, analyse the results and show that certain uncertainty methods can be used to decide how much we should trust the output of our networks (Section 5.3) and that we can improve upon our results by using calibrated models (Section 5.4). We show that these techniques work even when we consider domain shifts (Section 5.5) or noise (Section 5.6) in the input. For instance, when performing transfer learning on a network trained on Cityscapes to the Dark Zurich dataset, we validate that we can predict the specific cases of failure in segmentation well. We hope our work provides insight into existing segmentation networks and helps drive further research to ensure their trustworthiness. Figure 1 shows some examples of our approach where we use entropy to judge whether a pixel is likely to be misclassified. We note that simple entropy can identify the likely misclassified regions with high recall. Further detailed analysis is presented in Section 5.

2 Related Works

Semantic segmentation has been researched by the vision community for over a decade, and has been well documented in survey papers such as Guo et al. (2018); Hao et al. (2020). However, we will primarily concern ourselves with relatively recent works that use deep neural networks for performing this task. Among these, most earlier works, such as Chen et al. (2014); Long et al. (2015); Yu et al. (2017); Zhao et al. (2017); Chen et al. (2017); Yang et al. (2018), are convolutional in structure and generally make use of existing Convolutional Neural Networks (CNN) such as VGG (Simonyan & Zisserman, 2014), ResNet (He et al., 2016), ResNeXt (Xie et al., 2017), for feature extraction purposes followed by combining extracted features, possibly at multiple scales, in novel ways. Generally, the classification is done at a lower resolution than the input image and is upsampled back to the original dimensions near the end of the pipeline. The improvement in performance across these approaches mainly derives from coming up with new novel ways of pooling and combining the extracted features, such as the usage of Dilated Convolutions, Pyramid Pooling and Atrous Spatial Pyramids, among others.

Newer approaches such as Cheng et al. (2021); Xie et al. (2021); Strudel et al. (2021); Gu et al. (2022); Jain et al. (2023b;a), are based on Transformer networks introduced in Vaswani et al. (2017). Initially proposed for natural language processing tasks, Transformers also proved effective in computer vision. These approaches follow two major pipelines for extracting features from the input. Either they use CNN feature extractors, much like earlier works, followed by Transformer decoders for refinement. Alternatively, they use ViT-like (Dosovitskiy et al., 2020) architectures where the input image is divided into patches, which are directly fed to a Transformer encoder for feature generation, followed by a Transformer decoder and segmentation head.

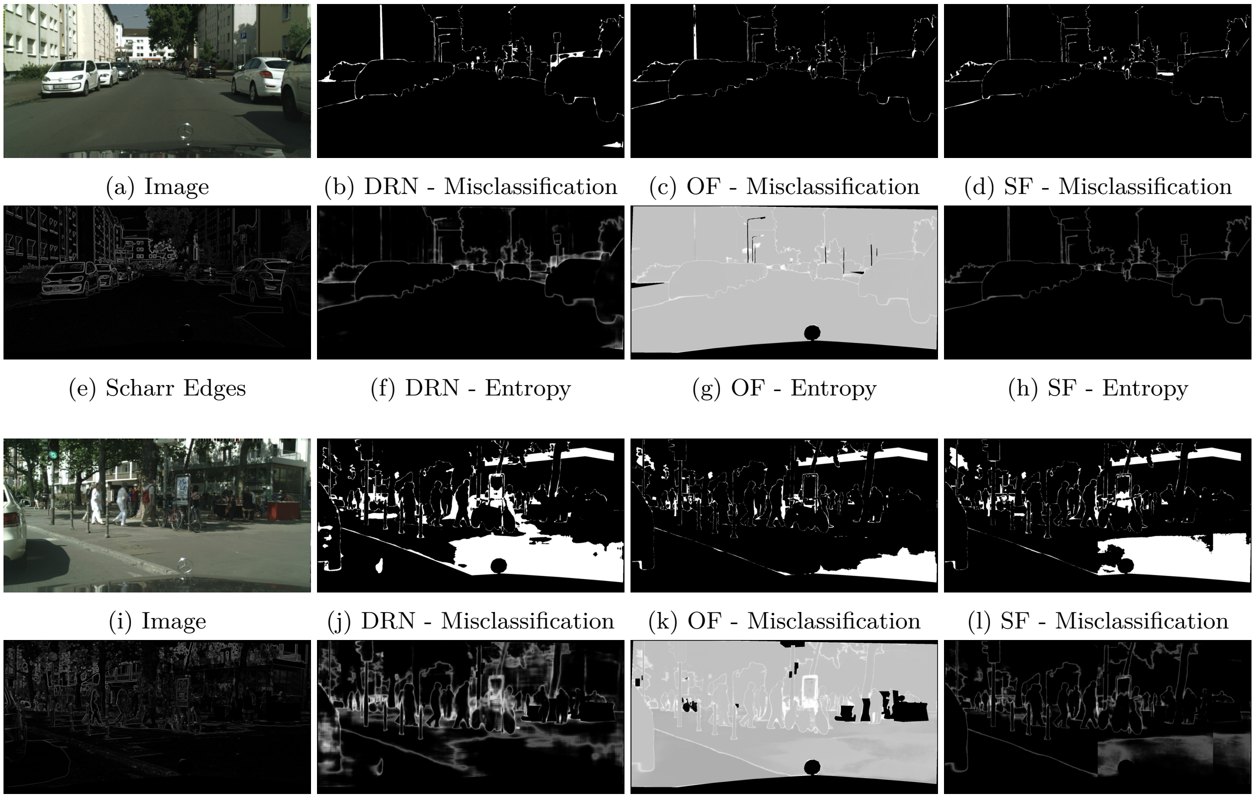

(a) Image (b) DRN - Misclassification (c) OF - Misclassification (d) SF - Misclassification

(e) Scharr Edges (f) DRN - Entropy (g) OF - Entropy (h) SF - Entropy

(i) Image (j) DRN - Misclassification (k) OF - Misclassification (l) SF - Misclassification

(m) Scharr Edges (n) DRN - Entropy (o) OF - Entropy (p) SF - Entropy

Figure 2: Comparison of misclassified pixels and entropy of DRN D-22 (DRN), OneFormer ConvNeXt-L (OF) and SegFormer B5 (SF) networks on a couple of Cityscapes validation images, along with the images themselves and edges detected using the Scharr operator. It is to be noted that OneFormer generally produces high entropy outputs, which cause most of the image to be grey. However, we can see that the highest entropy regions, in bright white, still correspond well to misclassified pixels.

We also consider how to extract uncertainty information from deep neural networks and refer to some existing works. Works like Deep Ensembles (Lakshminarayanan et al., 2017) and Bayesian Networks (Blundell et al., 2015) allow us to measure the uncertainty of predictions relatively easily, but they require special training procedures and are not applicable to already existing networks. However, Gal & Ghahramani (2016) shows that Dropout layers can be used to generate multiple predictions for a given input and thus allow us to compute a certain measure of model uncertainty. Similarly, Houlsby et al. (2011) proposed a metric originally meant for active learning but can also be used as an uncertainty measure for existing networks.

To the best of our knowledge, this type of work focusing on semantic segmentation has not been done earlier. Works such as Jammalamadaka et al. (2012); Parikh & Zitnick (2011); Vazhentsev et al. (2022); Xia et al. (2020); Rahman et al. (2022) are closest to our work. Vazhentsev et al. (2022) proposes and evaluates several uncertainty metrics for gauging the uncertainty of Transformer-based architectures and has similar goals of misclassification detection using uncertainty; however, the paper only explores these within the setting of Transformer architectures, and while most newer segmentation architectures are Transformer-based, older CNN-based networks are still used. Thus, we focus on making our evaluation and analysis as general as possible.

3 Failure Analysis

Before we develop a trust score or metric, we must first look at and try to understand the failure cases of our models. We consider a few standard segmentation networks - Dilated Residual Networks (Yu et al., 2017)

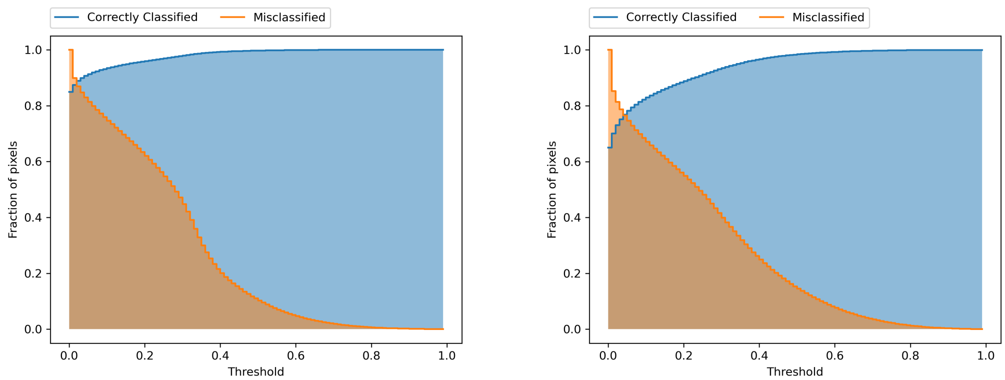

(a) DRN D-105, Cityscapes

(b) SegFormer B5, ADE20K

Figure 3: Cumulative histogram of entropy values for correctly classified (blue) and misclassified pixels (orange) for a couple of experimental settings. The graph is plotted such that if we choose any threshold value along the x-axis we can directly read what fraction of correctly classified and misclassified pixels are captured.

(DRN), OneFormer (Jain et al., 2023a) and SegFormer (Xie et al., 2021) and look at their outputs. We specifically choose a mix of older and newer networks for this since they are quite different architecturally and should allow us to focus on generalities rather than the peculiarities of any single architectural family. We use pre-trained weights on the Cityscapes dataset (Cordts et al., 2016) for all networks and observe their outputs on the validation set. Figures 2b to 2d and 2j to 2l highlight the misclassified pixels for the networks on a couple of such images. Black indicates correctly classified or ignored pixels, whereas white indicates misclassified pixels.

From the images, it is clear that OneFormer and SegFormer are better than DRN at segmenting images. Indeed, mIoU for DRN D-22, OneFormer ConvNeXT-L, and SegFormer B5 are 0.6790, 0.8287, and 0.8239, respectively. However, we note that the failure modes for the networks are very similar. All of these networks misclassify pixels in similar regions of the images. It is also evident that several of these misclassifications lie along the edges of various objects in the images. This makes intuitive sense since it can be challenging, even for humans, to assign the boundary pixels to a particular object exactly.

This naturally brings us to the question, *"Can we reasonably predict which pixels are most likely to be misclassified?"*. Even if we cannot accurately predict which pixels will be misclassified, we would like to have some measure of confidence in these classifications. Since we would like to apply whatever approach we come up with on existing networks without any re-training or finetuning, we need to consider what kind of information we can extract and use from just the images and their segmentation predictions since that is all we have during test time. Edge detection may seem an obvious first choice, as we have already established that several misclassified pixels lie along object boundaries. A better choice is some measure of uncertainty, such as entropy.

Figures 2e and 2m show the edges obtained when the Scharr filter is applied to the images. The gradient magnitudes thus obtained are scaled between $[0, 1]$, with 0 being black and 1 being white. All ignored pixels are also in black. Since the edges are obtained from just the image rather than the predictions, the network used does not matter. This already tells us that edge detection may not be particularly effective in predicting misclassifications, which depend on the segmentation network used. While some edges align well with the misclassifications, most are correctly classified, especially the edges within each object. The fact remains that only the edges that align with ground truth label boundaries are misclassified. Moreover, by its very nature, edge detection completely fails to capture any misclassified pixels within objects; this is especially evident in the second image (Figure 2m).

On the other hand, the simple entropy of predicted labels, as shown in Figures 2f to 2h and 2n to 2p, is far more aligned with the misclassifications. Similar to edges, the entropy is scaled between $[0, 1]$ for each image and ignored pixels are set to 0. Here, we see a marked difference between OneFormer and the other two networks; DRN and SegFormer provide very confident predictions and result in most pixels having very low entropy, whereas OneFormer's classifications are under-confident, resulting in most pixels having higher entropy. However, even then, at a glance, we notice that the highest entropy pixels align well with misclassifications.

For a more quantitative look, we plot the cumulative histogram of entropy values for correctly classified and misclassified pixels in Figure 3. The plot accumulates histogram counts for correctly classified pixels as the threshold increases and accumulates counts for misclassified pixels as it decreases. This allows us to directly read the percentage of correct and incorrect pixels predicted if we threshold entropy at any given value and consider anything below the threshold to be correctly classified and anything above it to be misclassified.

With these observations in mind, we focus on quantitative analysis of various uncertainty measures, which can be derived at test time, on pre-trained networks and consider how well they manage to predict misclassified pixels.

4 Uncertainty Metrics

We now describe the uncertainty metrics used for our experiments and how they are calculated. We only consider metrics that can be obtained purely at test time and those that work with nearly all neural networks. This rules out any approach for gauging uncertainty that requires us to change the network structure or fine-tune it. Specifically, we consider the following techniques.

- **Probability Scores -** Some of the simplest possible uncertainty metrics we can obtain involve directly using the highest probability scores output by the network (Hendrycks & Gimpel, 2016). We consider two different but related metrics. The first one is often called the Variation Ratio and is defined as follows:
$$\mathrm{VR} = 1 - p_m \tag{1}$$
where, $p_m = \max_{k=1}^{K}(p_k)$ represents the highest probability across all classes, and p_k represents the probability of a pixel belonging to class k.

  The second metric, Probability Margin, takes into account the difference between the highest and the second highest probability and is defined as:
$$\mathrm{PM} = 1 - \left\{ p_m - \max_{k=1, k \neq m}^{K} (p_k) \right\} \tag{2}$$

- **Entropy -** Another simple and possibly the most commonly used uncertainty metric we can obtain from a model. The only requirement is that the model outputs a probability distribution per pixel over all classes, which is true for nearly all (if not all) semantic segmentation models. Formally, the entropy for a single pixel is defined as:
$$\mathrm{H} = -\sum_{k=1}^{K} p_k \log p_k \tag{3}$$
where, K is the number of classes and p_k represents the probability of the pixel belonging to class k.

The above-mentioned techniques can be used with just a single output mask per image, but for metrics like BALD we need multiple outputs. To generate such outputs for each input image, we consider the following techniques.

- **Monte Carlo Dropout (MC Dropout) (Gal & Ghahramani, 2016) -** Typically, Dropout layers (Hinton et al., 2012) in neural networks are disabled during test time and replaced with a simple scaling of the features. MC Dropout utilises these layers to generate multiple predictions for the same image by keeping the Dropout layers active during test time. This introduces a source of randomness in the network, which allows it to produce different outputs for the same input on each forward pass. However, one drawback of the technique is that it can only be used with networks trained with Dropout layers.

- **Noise** - Yet another approach to obtaining multiple outputs is to introduce a tiny amount of random noise in the input, which perturbs the output. Like MC Dropout, this allows us to generate multiple predictions for the same input by using multiple forward passes (each with a different noise). For our purposes, we use zero mean Gaussian noise, with a small standard deviation.
- **Scaling** - Segmentation networks already use multi-scale inputs to improve their performance (Jain et al., 2023a; Yu et al., 2017). Essentially, it involves running forward passes on multiple scales of the input, which generate multiple segmentations for the same image. The networks can then scale back the outputs to the original resolution and average them to get better results than a single pass. We can, however, keep these generated masks for computing uncertainty.

Once we obtain multiple predictions for each input image, we can extract uncertainty information from these in the following manner.

- **Averaged Probability Scores** - Given multiple probability distributions over a pixel, we can take their mean to obtain a single representative probability distribution for said pixel. Mathematically we have:

$$\overline{p_k} = \frac{1}{N} \sum_{i=1}^{N} p_k^i \tag{4}$$

where $\overline{p_k}$ represents the average probability of a pixel belonging to class k, and p_k^i represents the probability of the pixel belonging to class k for the i^{th} prediction. N is the total number of predictions. Once we have the average probability distribution per pixel, we can compute Variation Ratio and Probability Margin values over them as follows:

$$\text{VR} = 1 - \overline{p_m}, \quad \text{where} \quad \overline{p_m} = \max_{k=1}^{K}(\overline{p_k}) \tag{5}$$

$$\text{PM} = 1 - \left\{ \overline{p_m} - \max_{k=1, i \neq m}^{K} (\overline{p_k}) \right\} \tag{6}$$

- **Averaged Entropy** - Similar to averaged probability scores, we can use Equation (4) to obtain the average probability distribution per pixel and compute entropy over it as:

$$\text{H} = -\sum_{k=1}^{K} \overline{p_k} \log \overline{p_k} \tag{7}$$

- **Variance** - Variance of the probability distribution has also been used as a measure of uncertainty in Bayesian settings (Gal et al., 2017; Smith & Gal, 2018). Since we have multiple predictions, we can compute the empirical variance of class k for any given pixel as:

$$\sigma_k^2 = \frac{1}{N} \sum_{i=1}^{N} (p_k^i - \overline{p_k})^2 \tag{8}$$

where, $\overline{p_k}$ is calculated as in eq. (4). To obtain a single value per pixel, we consider taking both the average as well as the maximum across across all classes.

- **Bayesian Active Learning by Disagreement (BALD)** (Houlsby et al., 2011) - Originally proposed as an acquisition function for selecting samples in a Bayesian active learning setting, BALD can also be used as an uncertainty metric. The BALD score is defined as:

$$\text{BALD} = -\sum_{k=1}^{K} \overline{p_k} \log \overline{p_k} + \frac{1}{N} \sum_{k=1, i=1}^{K, N} p_k^i \log p_k^i \tag{9}$$

where, $\overline{p_k}$ and p_k^i are same as defined earlier. Essentially, it checks the disagreement between the entropy of the expected prediction and the expected entropy across all predictions. Higher disagreement represents more uncertainty.

5 Experiments and Observation

In this section, we discuss the various experiments performed along with their results and observe the degree of correlation between existing uncertainty metrics and misclassifications in semantic image segmentation. We also look at how well we are able to capture misclassifications when there are domain shifts in the inputs or when the input is noisy. We also consider calibrating the models to improve our results further.

5.1 Datasets and Models

We consider the following datasets for our experiments, as they are quite standard for image segmentation tasks and the networks we have chosen provide pre-trained weights for these datasets.

- **Cityscapes (Cordts et al., 2016) -** The primary dataset used for our experiments consists of dashcam videos from cars in several German cities targeted towards understanding urban street scenes. The validation set is comprised of 500 finely annotated images of 2048×1024 resolution. Pixels in each image are annotated as belonging to one of 30 defined classes, of which 19 are considered for classification and evaluation. Any pixels not belonging to one of these classes are effectively ignored for evaluation purposes.

- **Dark Zurich (Sakaridis et al., 2019) -** A dataset analogous to Cityscapes with a small validation set of only 50 images with resolution of 1920×1080; it consists of urban scenes from the city of Zurich at night time as opposed to Cityscapes where the images are taken at day time. We use this dataset to check how well our metrics perform when there is a domain shift of the input.

- **ADE20K (Zhou et al., 2019) -** A rather large dataset with a validation set of 2000 images of varying resolutions. Unlike Cityscapes and Dark Zurich, ADE20K has a much larger number of segmentation classes, 150 and the images are not only from dashcam videos but cover a wide range of subjects.

We now describe the segmentation networks that were used in our experiments. We choose our models such that they range from small (DRN D-22) to large (OneFormer Swin-L) and cover a wide variety of architectures.

- **Dilated Residual Networks (Yu et al., 2017) -** Convolutional Neural Network (CNN) based on ResNet (He et al., 2016) but using Dilated Convolutions instead, which helps it achieve better performance in semantic segmentation tasks. We use the pre-trained weights for DRN D-22 and DRN D-105 variants provided by the authors for the Cityscapes dataset.

- **OneFormer (Jain et al., 2023a) -** Transformer-based architecture that utilises features from a backbone network and passes them through a Transformer decoder to get pixel-level classifications. We use pre-trained weights with ConvNeXt-L and Swin-L backbones on Cityscapes and ADE20K datasets, as provided by the authors.

- **SegFormer (Xie et al., 2021) -** Another Transformer-based architecture that uses a Hierarchical Transformer encoder and a Multi-Layer Perceptron (MLP) decoder. We use pre-trained weights of the B5 variant for Cityscapes and ADE20K datasets as provided by the authors.

5.2 Evaluation Metrics and Scenarios

In order to measure how well a particular uncertainty metric corresponds to misclassifications, we use Precision, Recall, Area Under the Receiver Operating Characteristic (AUROC), Area Under the Precision Recall Curve (AUPRC) and False Positive Rate at 95% True Positive Rate metrics. AUROC involves plotting the False Positive Rate against the True Positive Rate at different thresholds and then computing the area covered by the curve. Similarly AUPRC computes the area under the Precision Recall Curve at different thresholds. While AUROC and AUPRC consider multiple threshold values, we need to choose a single threshold value to binarise the uncertainty scores for computing Precision and Recall. Unfortunately, as seen in Figure 2, the scales of these uncertainty values can vary quite a lot across different models and even across different images for a single model. As such, we cannot use a single constant threshold value across all models or images. Therefore, we define a couple of processes to dynamically choose a threshold for each image. Both methods rely on the fact that the fraction of misclassified pixels is not very high.

1. For the first method, we check the ratio of predicted misclassified pixels to total pixels at multiple uniformly spaced threshold levels and select the threshold that causes the largest change in this value.

2. We note that the ratio of predicted misclassified pixels to total pixels increases as the threshold increases. For the second method, we specify a maximum value allowed for this ratio and choose the highest threshold, which results in a ratio lower than the specified value.

Before we discuss the results, we clarify the meaning of each scenario:

- **Base** - The simplest scenario where we only consider a single forward pass. As such, only Variation Ratio, Probability Margin and Entropy can be used as uncertainty metrics for this setting.
- **Noise** - The images are injected with a Gaussian noise of zero mean and 0.01 standard deviation. The noise is injected after normalizing the images. We use ten forward passes per image in this setting.
- **Scale** - This represents using multi-scaled inputs for generating multiple outputs. We use scales of $\{0.5, 0.75, 1.0, 1.25, 1.5\}$ for our purposes.
- **Drop** - MC Dropout is applied in this scenario. Since it requires the network to have Dropout layers, we did not use this technique with DRN. Similar to the Noise scenario, we use ten passes per image.

Before moving ahead, we would like to state that although a large number of experiments under various scenarios were performed, we only highlight some of those results for brevity and compactness in the following text. The complete set of results for all the experiments is provided in the appendix for this paper. Similarly, since we obtain the metrics for each pixel rather than each image, we consider both micro-averaging and macro-averaging over the images. However, we only show the micro-averaged results in this text and provide the rest in the appendix. The appendix also includes classwise results for several experiments.

5.3 Primary Analysis

As AUROC allows us to get a good overview of how our uncertainty metrics correlate with misclassification, we first look at these in Table 1 for the Cityscapes dataset. We observe that simple metrics like Entropy and Probability Scores perform better than more involved metrics such as Variance and BALD. We also look at the values of AUROC on ADE20K dataset in Table 2. The differences are smaller between various metrics on this dataset. Across both datasets the Scale scenario performs the best.

We show the AUPRC-Error, AUPRC-Success and False Positive Rate at 95% True Positive Rate results on the Cityscapes dataset using Entropy as an uncertainty metric in Table 3. AUPRC-Error denotes the AUPRC obtained when the misclassifications are treated as the positive class, whereas AUPRC-Success is

Table 1: Area under the Receiver Operating Characteristics (AUROC) on the Cityscapes dataset. We observe that we can obtain high AUROC scores even with simple uncertainty metrics such as Entropy.

Scenario	Var. Ratio	Prob. Margin	Entropy	Avg. Var.	Max. Var.	BALD
			DRN D-22			
Base	0.9118	0.9152	0.9205			
Noise	0.9119	0.9152	0.9205	0.7609	0.7614	0.8196
Scale	0.9410	**0.9414**	0.9398	0.8973	0.8976	0.9066
			OneFormer ConvNeXt-L			
Base	0.7265	0.7893	0.7089			
Noise	0.7334	0.7927	0.7153	0.6458	0.6323	0.6727
Scale	0.7647	**0.8305**	0.7350	0.7835	0.7637	0.8173
Drop	0.7471	0.8059	0.7278	0.7219	0.6994	0.7624
			SegFormer B5			
Base	0.8830	0.8892	0.8997			
Noise	0.8833	0.8896	0.9002	0.6972	0.6965	0.7520
Scale	0.9212	0.9245	**0.9290**	0.8678	0.8687	0.8947
Drop	0.8842	0.8904	0.9008	0.7677	0.7660	0.8255

Table 2: Area under the Receiver Operating Characteristics (AUROC) on the ADE20K dataset. While we do not perform as well as on Cityscapes our AUROC values are still reasonably good.

Scenario	Var. Ratio	Prob. Margin	Entropy	Avg. Var.	Max. Var.	BALD
			OneFormer ConvNeXt-L			
Base	0.6067	0.7048	0.5588			
Noise	0.6052	0.7039	0.5576	0.6328	0.6184	0.6218
Scale	0.6243	0.7285	0.5693	0.6880	0.6635	**0.7473**
Drop	0.6136	0.7151	0.5618	0.6732	0.6517	0.7359
			SegFormer B5			
Base	0.8000	0.8024	0.8113			
Noise	0.8003	0.8028	0.8115	0.7123	0.7116	0.7627
Scale	0.8356	0.8353	**0.8384**	0.7929	0.7929	0.8141
Drop	0.8016	0.8039	0.8125	0.7521	0.7520	0.7914

obtained when correctly classified pixels are treated as the positive class. Since all of our uncertainty metrics are normalized between $[0, 1]$ and higher values represent more uncertainty, we flip these values as $1 - x$ for calculating AUPRC-Success. Similar to AUROC, the Scale setting performs the best.

We now take a look at how well our first method for dynamic thresholding works. Table 4 shows the results of using the largest difference as a thresholding technique on the Cityscapes dataset. We use Entropy as the uncertainty metric. We observe that while we get very high recall rates, we also select quite a large fraction of pixels with values reaching as high as 40% for the Scale setting with DRN. As a result, precision suffers quite a bit in these cases. However, we will see later that this technique is useful when the network produces highly inaccurate outputs, such as when there is a domain shift in the input.

We now consider the performance of the second thresholding method. Table 5 shows the results for the same on the Cityscapes dataset. As expected, recall improves at the cost of precision across all scenarios when we increase the maximum fraction of pixels allowed. However, even with as few as 10% pixels, we can get 60-70% recall using Entropy as an uncertainty metric. Among the different scenarios, Scale performs better than the others, especially for Transformer-based networks.

Table 3: AUPRC-Error, AUPRC-Success, and FPR@95%TPR on the Cityscapes dataset using Entropy as the uncertainty metric.

Scenario	AUPRC-Error ↑	AUPRC-Success ↑	FPR@95%TPR ↓
	DRN D-22		
Base	0.4249	0.9953	25.15
Noise	0.4246	0.9953	25.15
Scale	**0.4469**	**0.9963**	**19.88**
	OneFormer ConvNeXt-L		
Base	0.1193	0.9847	80.34
Noise	0.1244	0.9844	**79.26**
Scale	**0.1424**	**0.9860**	79.61
Drop	0.1332	0.9853	79.91
	SegFormer B5		
Base	0.3840	0.9966	100.00
Noise	0.3826	0.9967	100.00
Scale	**0.4099**	**0.9975**	100.00
Drop	0.3843	0.9966	100.00

Table 4: Precision, Recall and F1 Score on Cityscapes dataset using largest difference as thresholding strategy. All of the results shown use Entropy as the uncertainty metric.

Scenario	Precision	Recall	F1 Score	Pixel %
		DRN D-22		
Base	**17.52**	95.04	**29.58**	28.94
Noise	**17.52**	95.05	**29.58**	28.95
Scale	13.04	**98.74**	23.04	40.38
		OneFormer ConvNeXt-L		
Base	14.13	81.30	24.07	18.40
Noise	**14.25**	80.60	**24.22**	18.08
Scale	12.11	82.76	21.13	21.84
Drop	13.76	**82.96**	23.60	19.28
		SegFormer B5		
Base	**21.43**	86.20	**34.33**	13.14
Noise	21.37	86.34	34.26	13.20
Scale	17.37	**92.46**	29.24	17.39
Drop	21.28	86.46	34.16	13.27

5.4 Calibration Experiments

In order to improve our scores, we also consider calibrating the networks we are using. We compute the Expected Calibration Error and Brier Score of all the networks tested and find that OneFormer, especially, is not well-calibrated. We use temperature scaling on the logits while computing softmax to counter this and generally find that our AUROC scores using Entropy as the uncertainty metric do improve on the calibrated models. This experiment indicates that considering the underlying causes for uncertainty, such as calibration, and fixing these can help further identify the misclassified pixels. We show the results of this experiment in Table 6. We use temperatures of 0.2 and 2 for OneFormer and SegFormer models respectively. We found that DRN models were already well calibrated and further temperature tuning was unnecessary.

Table 5: Precision and Recall on Cityscapes dataset using maximum percentage of pixels as thresholding strategy. All of the results shown use Entropy as the uncertainty metric.

Scenario	Max 5% pixels			Max 10% pixels			Max 15% pixels		
	Precision	Recall	Pixel %	Precision	Recall	Pixel %	Precision	Recall	Pixel %
				DRN D-22					
Base	**44.04**	39.76	4.82	34.80	63.64	9.75	28.11	76.42	14.50
Noise	44.02	39.75	4.82	34.79	63.64	9.76	28.12	76.45	14.50
Scale	43.68	39.53	4.83	35.26	63.98	9.68	28.67	**78.57**	14.62
				OneFormer ConNeXt-L					
Base	30.89	44.48	4.60	23.82	64.18	8.61	20.07	70.79	11.28
Noise	31.29	45.12	4.61	24.19	65.25	8.62	20.46	71.70	11.20
Scale	**31.49**	46.19	4.69	23.63	66.65	9.02	19.21	**73.98**	12.31
Drop	31.03	45.20	4.66	23.63	65.94	8.92	19.41	72.95	12.01
				SegFormer B5					
Base	36.61	54.78	4.89	26.09	74.94	9.38	22.42	82.52	12.03
Noise	36.49	54.55	4.88	26.04	74.84	9.39	22.36	82.56	12.06
Scale	**37.88**	56.12	4.84	26.49	78.44	9.67	20.75	**86.91**	13.68
Drop	36.61	54.74	4.88	26.05	74.96	9.40	22.31	82.68	12.10

Table 6: ECE, Brier Score (BS), AUROC, AUPRC-Error and AUPRC-Success for uncalibrated and calibrated models in Base setting with Entropy as uncertainty metric for the Cityscapes dataset.

Model	ECE ↓	BS ↓	AUROC ↑	AUPRC-Error ↑	AUPRC-Success ↑
			OneFormer ConvNeXT-L		
Uncalibrated	0.7887	0.8012	0.7089	0.1193	0.9847
Calibrated	**0.1173**	**0.0668**	**0.8387**	**0.2685**	**0.9885**
			SegFormer B5		
Uncalibrated	0.0631	0.0516	0.8997	**0.3840**	0.9966
Calibrated	**0.0282**	**0.0506**	**0.9357**	0.3382	**0.9975**

5.5 Domain Shift

In order to check whether these uncertainty metrics can capture misclassification in the case of input domain shift, we consider testing the models trained with the Cityscapes dataset on the Dark Zurich dataset. Dark Zurich is similar to Cityscapes in the sense that both include dashcam images from German cities. The major difference is that in Dark Zurich the images are taken during nighttime while in Cityscapes the images are taken during the day. This represents a natural domain shift one may encounter in the real world. Table 7 shows the results of using Cityscape- trained DRN and OneFormer models on the Dark Zurich dataset using Entropy as the uncertainty metric. The models perform poorly on this dataset, with mIoU of 0.0710 for DRN and 0.3994 for OneFormer. Even though the models perform poorly, we note that we can still use Entropy to get good Precision and Recall rates using the largest difference method for dynamic thresholding. We also note that using multiple scales generally performs better than other scenarios.

5.6 Noisy Inputs

We also consider introducing noise in the input images and observing how it affects our results. Effectively, this represents another form of domain shift. We introduce varying levels of noise in the input and check the performance of the networks on them. The noise introduced is Gaussian in nature with standard deviations of $\{5, 10, 25, 50\}$. The noise is introduced into the image before any preprocessing to ensure we do not subvert any mechanisms used by the networks to protect against such cases. Table 8 shows the AUROC values in this scenario on DRN D-22 and OneFormer ConvNeXt-L models. We also provide a visual example of the

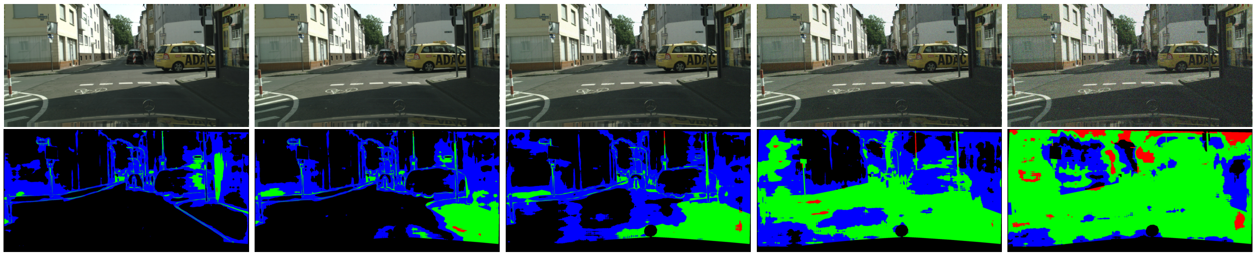

Figure 4: An example of how DRN misclassifies inputs when noise is added and how well entropy can capture it. From left to right, we have the original image followed by increasing amounts of noise added to it. The bottom row shows misclassified pixels with high entropy in green, misclassified pixels with low entropy in red and correctly classified pixels with high entropy in blue.

Table 7: Precision, Recall and AUROC on the Dark Zurich dataset, with Entropy as the uncertainty metric.

Scenario	Largest Difference				AUROC
	Precision	Recall	F1 Score	Pixel %	
		DRN D 22			
Base	68.92	80.93	74.44	77.21	0.6054
Noise	68.77	**80.95**	74.37	77.39	0.6024
Scale	**71.92**	79.24	**75.40**	72.45	**0.6680**
		OneFormer ConNeXt-L			
Base	38.41	56.71	45.80	42.67	0.5667
Noise	41.33	56.58	47.77	39.57	0.5641
Scale	**42.47**	**73.21**	**53.76**	49.82	**0.6377**
Drop	39.10	57.44	46.53	42.46	0.5755

Table 8: AUROC for increasing noise levels on the Cityscapes dataset for DRN and OneFormer models.

Scenario	DRN D-22	OneFormer ConvNeXt-L
Base	0.9205	0.7089
Noise 5	0.8554	0.6975
Noise 10	0.7866	0.7008
Noise 25	0.7156	0.6810
Noise 50	0.6427	0.6375

same in Figure 4. As can be seen with increasing noise levels, the outputs become highly inaccurate, but we can still capture most of these using Entropy as the uncertainty metric.

6 Conclusion

In this paper, we present a new form of analysis for semantic segmentation tasks focused on trusting the output of such networks during test time. Our work is primarily concerned with evaluating existing uncertainty metrics and seeing how well they correlate with and are able to capture misclassifications. Our analysis suggests that it is indeed possible to obtain valid evaluation measures that can be used to predict the test time performance of existing segmentation networks. We have shown that even simple measures such as Probability Margins and Entropy can be used as a proxy for capturing misclassified pixels with high recall rates. Because of their simplicity and generality, such tests can be used with nearly all existing architectures without any computational overhead and can help us know when the outputs are to be trusted. We believe that our work will provide new insights into the nature of semantic segmentation and help drive further research in evaluating the trustworthiness of these networks.

References

Charles Blundell, Julien Cornebise, Koray Kavukcuoglu, and Daan Wierstra. Weight uncertainty in neural network. In *International conference on machine learning*, pp. 1613–1622. PMLR, 2015.

Liang-Chieh Chen, George Papandreou, Iasonas Kokkinos, Kevin Murphy, and Alan L Yuille. Semantic image segmentation with deep convolutional nets and fully connected crfs. *arXiv preprint arXiv:1412.7062*, 2014.

Liang-Chieh Chen, George Papandreou, Iasonas Kokkinos, Kevin Murphy, and Alan L Yuille. Deeplab: Semantic image segmentation with deep convolutional nets, atrous convolution, and fully connected crfs. *IEEE transactions on pattern analysis and machine intelligence*, 40(4):834–848, 2017.

Bowen Cheng, Alex Schwing, and Alexander Kirillov. Per-pixel classification is not all you need for semantic segmentation. *Advances in Neural Information Processing Systems*, 34:17864–17875, 2021.

Marius Cordts, Mohamed Omran, Sebastian Ramos, Timo Rehfeld, Markus Enzweiler, Rodrigo Benenson, Uwe Franke, Stefan Roth, and Bernt Schiele. The cityscapes dataset for semantic urban scene understanding. In *Proceedings of the IEEE conference on computer vision and pattern recognition*, pp. 3213–3223, 2016.

Alexey Dosovitskiy, Lucas Beyer, Alexander Kolesnikov, Dirk Weissenborn, Xiaohua Zhai, Thomas Unterthiner, Mostafa Dehghani, Matthias Minderer, Georg Heigold, Sylvain Gelly, et al. An image is worth 16x16 words: Transformers for image recognition at scale. *arXiv preprint arXiv:2010.11929*, 2020.

Yarin Gal and Zoubin Ghahramani. Dropout as a bayesian approximation: Representing model uncertainty in deep learning. In *international conference on machine learning*, pp. 1050–1059. PMLR, 2016.

Yarin Gal, Riashat Islam, and Zoubin Ghahramani. Deep bayesian active learning with image data. In *International conference on machine learning*, pp. 1183–1192. PMLR, 2017.

Jakob Gawlikowski, Cedrique Rovile Njieutcheu Tassi, Mohsin Ali, Jongseok Lee, Matthias Humt, Jianxiang Feng, Anna Kruspe, Rudolph Triebel, Peter Jung, Ribana Roscher, et al. A survey of uncertainty in deep neural networks. *Artificial Intelligence Review*, 56(Suppl 1):1513–1589, 2023.

Will Grathwohl, Kuan-Chieh Wang, Jörn-Henrik Jacobsen, David Duvenaud, Mohammad Norouzi, and Kevin Swersky. Your classifier is secretly an energy based model and you should treat it like one. *arXiv preprint arXiv:1912.03263*, 2019.

Jiaqi Gu, Hyoukjun Kwon, Dilin Wang, Wei Ye, Meng Li, Yu-Hsin Chen, Liangzhen Lai, Vikas Chandra, and David Z Pan. Multi-scale high-resolution vision transformer for semantic segmentation. In *Proceedings of the IEEE/CVF Conference on Computer Vision and Pattern Recognition*, pp. 12094–12103, 2022.

Yanming Guo, Yu Liu, Theodoros Georgiou, and Michael S Lew. A review of semantic segmentation using deep neural networks. *International journal of multimedia information retrieval*, 7:87–93, 2018.

Shijie Hao, Yuan Zhou, and Yanrong Guo. A brief survey on semantic segmentation with deep learning. *Neurocomputing*, 406:302–321, 2020.

Kaiming He, Xiangyu Zhang, Shaoqing Ren, and Jian Sun. Deep residual learning for image recognition. In *Proceedings of the IEEE conference on computer vision and pattern recognition*, pp. 770–778, 2016.

Dan Hendrycks and Kevin Gimpel. A baseline for detecting misclassified and out-of-distribution examples in neural networks. *arXiv preprint arXiv:1610.02136*, 2016.

Geoffrey E Hinton, Nitish Srivastava, Alex Krizhevsky, Ilya Sutskever, and Ruslan R Salakhutdinov. Improving neural networks by preventing co-adaptation of feature detectors. *arXiv preprint arXiv:1207.0580*, 2012.

Neil Houlsby, Ferenc Huszár, Zoubin Ghahramani, and Máté Lengyel. Bayesian active learning for classification and preference learning. *arXiv preprint arXiv:1112.5745*, 2011.

Jitesh Jain, Jiachen Li, Mang Tik Chiu, Ali Hassani, Nikita Orlov, and Humphrey Shi. Oneformer: One transformer to rule universal image segmentation. In *Proceedings of the IEEE/CVF Conference on Computer Vision and Pattern Recognition*, pp. 2989–2998, 2023a.

Jitesh Jain, Anukriti Singh, Nikita Orlov, Zilong Huang, Jiachen Li, Steven Walton, and Humphrey Shi. Semask: Semantically masked transformers for semantic segmentation. In *Proceedings of the IEEE/CVF International Conference on Computer Vision*, pp. 752–761, 2023b.

Nataraj Jammalamadaka, Andrew Zisserman, Marcin Eichner, Vittorio Ferrari, and CV Jawahar. Has my algorithm succeeded? an evaluator for human pose estimators. In *Computer Vision–ECCV 2012: 12th European Conference on Computer Vision, Florence, Italy, October 7-13, 2012, Proceedings, Part III 12*, pp. 114–128. Springer, 2012.

Balaji Lakshminarayanan, Alexander Pritzel, and Charles Blundell. Simple and scalable predictive uncertainty estimation using deep ensembles. *Advances in neural information processing systems*, 30, 2017.

Jonathan Long, Evan Shelhamer, and Trevor Darrell. Fully convolutional networks for semantic segmentation. In *Proceedings of the IEEE conference on computer vision and pattern recognition*, pp. 3431–3440, 2015.

Devi Parikh and C Lawrence Zitnick. Finding the weakest link in person detectors. In *CVPR 2011*, pp. 1425–1432. IEEE, 2011.

Quazi Marufur Rahman, Niko Sünderhauf, Peter Corke, and Feras Dayoub. Fsnet: A failure detection framework for semantic segmentation. *IEEE Robotics and Automation Letters*, 7(2):3030–3037, 2022.

Christos Sakaridis, Dengxin Dai, and Luc Van Gool. Guided curriculum model adaptation and uncertainty-aware evaluation for semantic nighttime image segmentation. In *Proceedings of the IEEE/CVF International Conference on Computer Vision*, pp. 7374–7383, 2019.

Karen Simonyan and Andrew Zisserman. Very deep convolutional networks for large-scale image recognition. *arXiv preprint arXiv:1409.1556*, 2014.

Lewis Smith and Yarin Gal. Understanding measures of uncertainty for adversarial example detection. *arXiv preprint arXiv:1803.08533*, 2018.

Robin Strudel, Ricardo Garcia, Ivan Laptev, and Cordelia Schmid. Segmenter: Transformer for semantic segmentation. In *Proceedings of the IEEE/CVF international conference on computer vision*, pp. 7262–7272, 2021.

Ashish Vaswani, Noam Shazeer, Niki Parmar, Jakob Uszkoreit, Llion Jones, Aidan N Gomez, Łukasz Kaiser, and Illia Polosukhin. Attention is all you need. *Advances in neural information processing systems*, 30, 2017.

Artem Vazhentsev, Gleb Kuzmin, Artem Shelmanov, Akim Tsvigun, Evgenii Tsymbalov, Kirill Fedyanin, Maxim Panov, Alexander Panchenko, Gleb Gusev, Mikhail Burtsev, et al. Uncertainty estimation of transformer predictions for misclassification detection. In *Proceedings of the 60th Annual Meeting of the Association for Computational Linguistics (Volume 1: Long Papers)*, pp. 8237–8252, 2022.

Yingda Xia, Yi Zhang, Fengze Liu, Wei Shen, and Alan L Yuille. Synthesize then compare: Detecting failures and anomalies for semantic segmentation. In *Computer Vision–ECCV 2020: 16th European Conference, Glasgow, UK, August 23–28, 2020, Proceedings, Part I 16*, pp. 145–161. Springer, 2020.

Enze Xie, Wenhai Wang, Zhiding Yu, Anima Anandkumar, Jose M Alvarez, and Ping Luo. Segformer: Simple and efficient design for semantic segmentation with transformers. *Advances in Neural Information Processing Systems*, 34:12077–12090, 2021.

Saining Xie, Ross Girshick, Piotr Dollár, Zhuowen Tu, and Kaiming He. Aggregated residual transformations for deep neural networks. In *Proceedings of the IEEE conference on computer vision and pattern recognition*, pp. 1492–1500, 2017.

Maoke Yang, Kun Yu, Chi Zhang, Zhiwei Li, and Kuiyuan Yang. Denseaspp for semantic segmentation in street scenes. In *Proceedings of the IEEE conference on computer vision and pattern recognition*, pp. 3684–3692, 2018.

Fisher Yu, Vladlen Koltun, and Thomas Funkhouser. Dilated residual networks. In *Proceedings of the IEEE conference on computer vision and pattern recognition*, pp. 472–480, 2017.

Hengshuang Zhao, Jianping Shi, Xiaojuan Qi, Xiaogang Wang, and Jiaya Jia. Pyramid scene parsing network. In *Proceedings of the IEEE conference on computer vision and pattern recognition*, pp. 2881–2890, 2017.

Bolei Zhou, Hang Zhao, Xavier Puig, Tete Xiao, Sanja Fidler, Adela Barriuso, and Antonio Torralba. Semantic understanding of scenes through the ade20k dataset. *International Journal of Computer Vision*, 127:302–321, 2019.

A Cityscapes and ADE20K

First, we provide all results related to Cityscapes and ADE20K datasets. We provide results for Dark Zurich in a separate section, as experiments on it involve input domain shift. Table 9 collates all the performance metrics for the Base setting of all networks. We compute Mean Intersection Over Union (mIoU), Expected Calibration Error (ECE) and Brier Score (BS). For all of the metrics, we show both micro-averaged (μ Avg.) as well as macro-averaged (M Avg.) results.

As expected, DRN performs the worst among all the models, while OneFormer and SegFormer perform much better. We also note that DRN and SegFormer are relatively well-calibrated, but OneFormer is not. Results on Cityscapes are much better than on ADE20K since the latter is a much more challenging dataset with more variety and a much larger number of classes.

Table 9: Micro and macro-averaged (μ and M, respectively) Mean Intersection Over Union (mIoU), Expected Calibration Error (ECE) and Brier Score (BS) on Cityscapes and ADE20K datasets.

Model	mIoU ↑		ECE ↓		BS ↓	
	μ Avg.	M Avg.	μ Avg.	M Avg.	μ Avg.	M Avg.
			Cityscapes			
DRN D-22	0.6790	0.5479	0.0380	0.0177	0.0808	0.0824
DRN D-105	0.7551	0.6330	**0.0337**	0.0171	0.0617	0.0631
OneFormer ConvNeXt-L	0.8287	0.6733	0.7887	0.8383	0.8012	0.8011
OneFormer Swin-L	**0.8288**	0.6682	0.7973	0.8400	0.8034	0.8034
SegFormer B5	0.8239	**0.6875**	0.0631	**0.0160**	**0.0516**	**0.0524**
			ADE20K			
OneFormer ConvNeXt-L	0.5684	0.4854	0.8753	0.8195	0.9690	0.9686
OneFormer Swin-L	**0.5698**	**0.4921**	0.8948	0.8261	0.9689	0.9687
SegFormer B5	0.5100	0.4434	**0.1051**	**0.1068**	**0.2646**	**0.2845**

Table 10 and Table 11 show the Area Under Receiver Operating Characteristic (AUROC) as well as the Precision, Recall and fraction of selected pixels on Cityscapes and ADE20K datasets, respectively.

We observe that in most cases, Scale seems to provide the best AUROC and Recall, while Noise generally provides good Precision. However, in most cases, Base comes quite close to these values and has the advantage of being computationally cheaper. We also note that simpler metrics such as Variation Ratio, Probability Margin and Entropy are often better than or very close to more involved metrics such as Variance and BALD. The Recall values often reach higher than 90% for Cityscapes and 70% for ADE20K, although often at the cost of selecting too many pixels in the image.

Table 10: Micro and macro-averaged (μ and M, respectively) Area Under Receiver Operating Characteristic (AUROC) and Precision, Recall and the fraction of pixels selected for largest difference thresholding on the Cityscapes dataset.

Scenario	Uncertainty Metric	AUROC ↑		Largest Difference Thresholding					
				Precision ↑		Recall ↑		Pixel %	
		μ Avg.	M Avg.	μ Avg.	M Avg.	μ Avg.	M Avg.	μ Avg.	M Avg.
				DRN D-22					
Base	Var. Ratio	0.9118	0.9277	21.10	20.18	92.13	94.71	23.29	23.51
	Prob. Margin	0.9152	0.9302	19.71	18.84	93.31	95.62	25.26	25.48
	Entropy	0.9205	0.9337	17.52	16.74	95.04	96.89	28.94	29.21
Noise	Var. Ratio	0.9119	0.9278	21.10	20.18	92.15	94.73	23.30	23.52
	Prob. Margin	0.9152	0.9303	19.71	18.85	93.32	95.63	25.26	25.49
	Entropy	0.9205	0.9337	17.52	16.74	95.05	96.90	28.95	29.22
	Avg. Var.	0.7609	0.7722	**37.97**	**36.82**	57.26	59.58	08.04	08.13
	Max. Var.	0.7614	0.7724	37.71	36.55	57.42	59.71	08.12	08.21
	BALD	0.8196	0.8276	29.28	28.36	72.32	73.90	13.18	13.30
Scale	Var. Ratio	0.9410	**0.9466**	15.90	15.22	97.74	98.46	32.80	33.08
	Prob. Margin	**0.9414**	0.9465	14.80	14.19	98.14	98.76	35.36	35.66
	Entropy	0.9398	0.9444	13.04	12.52	**98.74**	**99.19**	40.38	40.72
	Avg. Var.	0.8973	0.8998	23.50	22.51	91.38	92.38	20.74	20.95
	Max. Var.	0.8976	0.8995	23.18	22.20	91.69	92.65	21.11	21.31
	BALD	0.9066	0.9075	16.49	15.82	96.37	97.10	31.17	31.44
				DRN D-105					
Base	Var. Ratio	0.8939	0.9206	23.04	22.19	85.84	90.61	14.76	14.87
	Prob. Margin	0.8995	0.9247	21.77	20.94	87.36	91.77	15.90	16.02
	Entropy	0.9094	0.9322	19.75	18.95	89.88	93.64	18.03	18.17
Noise	Var. Ratio	0.8949	0.9209	23.09	22.22	86.03	90.70	14.76	14.87
	Prob. Margin	0.9004	0.9250	21.82	20.98	87.54	91.84	15.90	16.01
	Entropy	0.9103	0.9325	19.79	18.98	90.05	93.70	18.03	18.16
	Avg. Var.	0.7471	0.7666	**39.53**	**38.65**	52.68	56.64	05.28	05.34
	Max. Var.	0.7472	0.7664	39.46	38.56	52.71	56.61	05.29	05.36
	BALD	0.8077	0.8249	32.48	31.63	66.59	70.05	08.12	08.21
Scale	Var. Ratio	0.9341	0.9474	19.48	18.60	93.73	95.92	19.07	19.21
	Prob. Margin	0.9366	0.9490	18.33	17.51	94.52	96.48	20.43	20.57
	Entropy	**0.9400**	**0.9509**	16.45	15.71	**95.79**	**97.33**	23.07	23.23
	Avg. Var.	0.8893	0.9007	27.81	26.58	84.51	87.00	12.04	12.15
	Max. Var.	0.8900	0.9009	27.59	26.37	84.74	87.17	12.17	12.28
	BALD	0.9111	0.9197	20.60	19.70	91.20	93.16	17.54	17.67
				OneFormer ConvNeXt-L					
Base	Var. Ratio	0.7265	0.8822	15.02	16.52	84.68	87.75	18.03	18.17
	Prob. Margin	0.7893	0.9073	14.37	15.63	89.19	91.32	19.84	19.98
	Entropy	0.7089	0.8569	14.13	16.23	81.30	84.88	18.40	18.65
Noise	Var.Ratio	0.7334	0.8851	15.04	16.66	84.72	87.85	18.00	18.13
	Prob. Margin	0.7927	0.9087	14.15	15.72	89.07	91.37	20.12	20.25
	Entropy	0.7153	0.8612	14.25	16.54	80.60	85.05	18.08	18.21
	Avg. Var.	0.6458	0.6474	18.71	28.78	34.52	35.06	05.90	05.99
	Max. Var.	0.6323	0.6324	17.11	27.49	31.93	32.20	05.97	06.05
	BALD	0.6727	0.6742	20.21	**29.16**	40.01	40.55	06.33	06.42
Scale	Var. Ratio	0.7647	0.8972	12.96	14.53	88.64	90.63	21.87	22.06
	Prob. Margin	**0.8305**	**0.9215**	12.58	13.53	**92.36**	**93.71**	23.46	23.68
	Entropy	0.7350	0.8736	12.11	14.36	82.76	87.42	21.84	21.90

	Avg. Var.	0.7835	0.7880	16.78	21.70	65.40	67.80	12.46	12.54
	Max. Var.	0.7637	0.7677	15.75	20.82	62.04	64.34	12.59	12.67
	BALD	0.8173	0.8213	17.66	21.76	71.71	74.12	12.98	13.05
Drop	Var. Ratio	0.7471	0.8936	14.89	15.82	85.54	89.39	18.36	18.44
	Prob. Margin	0.8059	0.9166	13.51	14.47	91.12	93.09	21.56	21.71
	Entropy	0.7278	0.8712	13.76	15.12	82.96	87.21	19.28	19.40
	Avg. Var.	0.7219	0.7264	21.08	27.12	49.93	52.42	07.57	07.68
	Max. Var.	0.6994	0.7023	19.55	25.98	45.49	47.68	07.44	07.54
	BALD	0.7624	0.7667	**21.71**	27.02	58.30	60.90	08.58	08.69
				OneFormer Swin-L					
Base	Var. Ratio	0.7379	0.8909	13.68	15.60	86.62	89.80	20.24	20.37
	Prob. Margin	0.7937	0.9127	13.30	14.59	89.82	92.61	21.57	21.72
	Entropy	0.7238	0.8677	13.57	15.52	82.85	86.61	19.51	19.73
Noise	Var.Ratio	0.7432	0.8927	14.34	15.84	86.49	89.67	19.28	19.48
	Prob. Margin	0.7976	0.9139	13.76	14.87	90.09	92.60	20.93	21.10
	Entropy	0.7288	0.8709	13.95	15.60	83.60	87.08	19.15	19.39
	Avg. Var.	0.6603	0.6611	23.56	29.87	36.01	36.33	04.88	05.00
	Max. Var.	0.6467	0.6463	22.08	28.63	33.36	33.46	04.83	04.95
	BALD	0.6866	0.6874	**25.56**	**30.50**	41.36	41.61	05.17	05.24
Scale	Var. Ratio	0.7816	0.9109	12.76	13.84	89.92	92.58	22.52	22.69
	Prob. Margin	**0.8415**	**0.9304**	11.87	12.90	**93.29**	**95.15**	25.12	25.40
	Entropy	0.7557	0.8951	12.30	13.65	87.69	90.83	22.78	22.95
	Avg. Var.	0.8093	0.8159	19.67	22.86	70.28	71.57	11.42	11.59
	Max. Var.	0.7929	0.7985	18.86	22.18	67.53	68.59	11.44	11.61
	BALD	0.8352	0.8421	20.03	22.73	75.31	76.74	12.02	12.20
Drop	Var. Ratio	0.7543	0.8972	13.39	14.67	87.99	90.76	20.99	21.20
	Prob. Margin	0.8078	0.9179	12.95	14.15	90.91	93.25	22.43	22.68
	Entropy	0.7396	0.8779	12.60	14.31	85.42	88.66	21.65	21.85
	Avg. Var.	0.7211	0.7397	23.02	28.08	49.79	53.67	06.91	07.04
	Max. Var.	0.6994	0.7164	21.31	27.09	45.57	49.20	06.83	07.01
	BALD	0.7593	0.7765	24.27	28.27	57.69	61.29	07.60	07.69
				SegFormer B5					
Base	Var. Ratio	0.8830	0.9087	24.60	24.07	82.10	86.94	10.90	10.95
	Prob. Margin	0.8892	0.9142	23.40	22.87	83.65	88.29	11.68	11.73
	Entropy	0.8997	0.9234	21.43	20.89	86.20	90.47	13.14	13.20
Noise	Var.Ratio	0.8833	0.9089	24.53	24.00	82.22	87.02	10.95	11.00
	Prob. Margin	0.8896	0.9143	23.33	22.81	83.77	88.37	11.73	11.78
	Entropy	0.9002	0.9236	21.37	20.84	86.34	90.55	13.20	13.26
	Avg. Var.	0.6972	0.7147	**40.19**	**40.11**	41.61	45.11	03.38	03.40
	Max. Var.	0.6965	0.7136	40.18	40.07	41.46	44.90	03.37	03.39
	BALD	0.7520	0.7697	34.08	34.03	53.80	57.30	05.16	05.19
Scale	Var. Ratio	0.9212	0.9391	20.33	19.77	90.13	93.35	14.48	14.56
	Prob. Margin	0.9245	0.9418	19.21	18.67	91.02	94.10	15.48	15.56
	Entropy	**0.9290**	**0.9459**	17.37	16.85	**92.46**	**95.29**	17.39	17.48
	Avg. Var.	0.8678	0.8826	28.23	27.55	78.95	81.98	09.13	09.19
	Max. Var.	0.8687	0.8832	28.04	27.36	79.20	82.18	09.23	09.28
	BALD	0.8947	0.9091	21.36	20.81	86.42	89.33	13.22	13.28
Drop	Var. Ratio	0.8842	0.9097	24.44	23.91	82.38	87.17	11.01	11.06
	Prob. Margin	0.8904	0.9151	23.24	22.72	83.92	88.50	11.80	11.85
	Entropy	0.9008	0.9242	21.28	20.74	86.46	90.66	13.27	13.33
	Avg. Var.	0.7677	0.7931	37.02	36.66	56.64	61.71	05.00	05.02
	Max. Var.	0.7660	0.7915	37.06	36.69	56.31	61.38	04.96	04.98
	BALD	0.8255	0.8519	28.97	28.73	70.12	75.25	07.91	07.93

Table 11: Micro and macro-averaged (μ and M, respectively) Area Under Receiver Operating Characteristic (AUROC) and Precision, Recall and the fraction of pixels selected for largest difference thresholding on the ADE20K dataset.

Scenario	Uncertainty Metric	AUROC ↑		Largest Difference Thresholding					
				Precision ↑		Recall ↑		Pixel %	
		μ Avg.	M Avg.	μ Avg.	M Avg.	μ Avg.	M Avg.	μ Avg.	M Avg.
				OneFormer ConvNeXt-L					
Base	Var. Ratio	0.6067	0.6941	25.45	28.92	50.31	63.73	29.11	30.34
	Prob. Margin	0.7048	0.7750	25.15	29.12	63.92	75.96	37.43	38.25
	Entropy	0.5588	0.6164	23.07	27.39	41.38	54.30	26.42	27.64
Noise	Var. Ratio	0.6052	0.6927	25.73	28.89	50.62	63.82	28.97	30.43
	Prob. Margin	0.7039	0.7727	25.48	29.24	63.66	75.54	36.79	37.66
	Entropy	0.5576	0.6151	23.34	27.23	41.43	54.34	26.13	27.57
	Avg. Var.	0.6328	0.6235	**30.67**	**35.27**	41.61	45.27	19.98	22.40
	Max. Var.	0.6184	0.6084	29.52	34.66	38.94	42.18	19.42	21.76
	BALD	0.6218	0.6672	26.34	29.24	54.24	58.38	30.32	33.04
Scale	Var. Ratio	0.6243	0.7078	24.23	28.00	52.29	65.56	31.78	32.76
	Prob. Margin	0.7285	**0.7883**	24.87	28.95	65.42	76.88	38.74	39.19
	Entropy	0.5693	0.6304	22.37	26.39	42.37	55.78	27.89	29.02
	Avg. Var.	0.6880	0.6728	27.69	30.54	61.78	66.51	32.85	35.02
	Max. Var.	0.6635	0.6489	26.92	29.84	58.47	62.64	31.98	34.25
	BALD	**0.7473**	0.7279	28.66	30.16	**73.48**	**77.93**	37.76	39.69
Drop	Var. Ratio	0.6136	0.6956	25.19	28.55	50.22	64.06	29.36	30.82
	Prob. Margin	0.7151	0.7778	25.10	29.06	63.51	76.03	37.26	38.10
	Entropy	0.5618	0.6169	22.72	26.59	40.91	54.33	26.51	27.99
	Avg. Var.	0.6732	0.6636	29.53	33.02	54.03	59.30	26.95	29.28
	Max. Var.	0.6517	0.6415	28.65	32.46	50.24	54.95	25.82	28.23
	BALD	0.7359	0.7258	29.66	31.50	68.32	74.11	33.92	36.23
				OneFormer Swin-L					
Base	Var. Ratio	0.6115	0.6977	24.79	28.04	52.66	64.95	30.16	31.21
	Prob. Margin	0.7066	0.7770	25.18	28.13	66.49	76.84	37.49	38.22
	Entropy	0.5661	0.6222	22.96	26.26	43.63	55.65	26.97	28.53
Noise	Var. Ratio	0.6110	0.6958	24.86	27.82	53.28	65.05	30.42	31.46
	Prob. Margin	0.7066	0.7748	24.83	27.98	65.73	76.59	37.58	38.38
	Entropy	0.5652	0.6208	22.82	26.20	43.62	55.28	27.13	28.37
	Avg. Var.	0.6331	0.6281	28.40	**34.11**	43.92	47.86	21.95	24.05
	Max. Var.	0.6180	0.6114	27.42	33.52	40.58	44.08	21.01	23.09
	BALD	0.6510	0.6806	26.38	29.88	57.68	62.16	31.04	33.33
Scale	Var. Ratio	0.6296	0.7142	23.84	27.27	55.82	67.39	33.23	33.60
	Prob. Margin	0.7322	**0.7933**	24.05	27.69	68.38	78.83	40.37	40.47
	Entropy	0.5742	0.6358	21.99	25.40	45.23	57.34	29.20	30.27
	Avg. Var.	0.6994	0.6891	27.97	30.37	64.48	68.74	32.72	34.31
	Max. Var.	0.6735	0.6643	26.78	29.50	60.42	64.77	32.02	33.75
	BALD	**0.7563**	0.7427	28.37	29.68	**74.23**	**79.18**	37.15	38.73
Drop	Var. Ratio	0.6173	0.7005	24.31	27.57	53.69	65.76	31.35	32.33
	Prob. Margin	0.7156	0.7804	24.41	28.04	65.93	76.85	38.34	38.83
	Entropy	0.5693	0.6241	22.34	25.76	43.40	55.83	27.57	28.91
	Avg. Var.	0.6665	0.6565	27.86	31.72	55.14	59.57	28.10	30.11
	Max. Var.	0.6459	0.6333	26.98	31.18	51.19	54.98	26.93	28.93

	BALD	0.7302	0.7182	**28.76**	30.76	69.12	73.75	34.11	35.92
				SegFormer B5					
Base	Var. Ratio	0.8000	0.8388	35.54	33.27	80.01	87.38	36.81	38.62
	Prob. Margin	0.8024	0.8397	34.56	32.45	81.51	88.36	38.56	40.28
	Entropy	0.8113	0.8484	32.20	30.34	84.63	90.97	42.96	44.99
Noise	Var. Ratio	0.8356	0.8628	31.86	30.41	88.13	93.03	45.22	46.72
	Prob. Margin	0.8353	0.8615	30.93	29.67	88.88	93.51	46.97	48.33
	Entropy	**0.8384**	**0.8661**	28.80	27.87	**90.24**	**94.82**	51.21	52.85
	Avg. Var.	0.7929	0.8096	39.47	37.55	77.79	83.11	32.22	33.33
	Max. Var.	0.7929	0.8089	39.28	37.40	78.06	83.31	32.48	33.60
	BALD	0.8141	0.8266	32.97	31.46	86.96	91.18	43.11	44.50
Scale	Var. Ratio	0.8003	0.8388	35.55	33.26	80.02	87.38	36.79	38.59
	Prob. Margin	0.8028	0.8397	34.57	32.44	81.51	88.35	38.54	40.24
	Entropy	0.8115	0.8483	32.12	30.34	84.27	90.91	42.89	44.93
	Avg. Var.	0.7123	0.7490	**48.46**	**45.09**	52.74	61.89	17.79	19.46
	Max. Var.	0.7116	0.7483	48.38	45.03	52.65	61.80	17.79	19.45
	BALD	0.7627	0.7952	41.45	38.38	68.51	76.96	27.02	29.59
Drop	Var. Ratio	0.8016	0.8398	35.32	33.08	80.47	87.70	37.24	39.05
	Prob. Margin	0.8039	0.8407	34.34	32.26	81.92	88.65	38.99	40.71
	Entropy	0.8125	0.8491	31.92	30.16	84.70	91.18	43.37	45.43
	Avg. Var.	0.7521	0.7955	44.41	41.56	63.76	73.73	23.47	24.96
	Max. Var.	0.7520	0.7955	44.35	41.52	63.85	73.85	23.54	25.04
	BALD	0.7914	0.8299	36.50	34.17	78.07	86.38	34.96	37.22

We also show the Area Under Precision Recall Curve (AUPRC) and False Positive Rate at 95% True Positive Rate (FPR@95%TPR) for selected models on the Cityscapes dataset in Table 12. For AUPRC we show both AUPRC Error and Success. In AUPRC-Error the misclassified pixels are treated as the positive class whereas in AUPRC-Success correctly classified pixels are treated as the positive class. We observe that much like in the case of AUROC, Scale setting peforms the best.

Table 12: Micro and macro-averaged (μ and M, respectively) Area Under Precision Recall Curve (AUPRC) and False Positive Rate at 95% True Positive Rate (FPR@95%TPR) on the Cityscapes dataset.

Scenario	Uncertainty Metric	AUPRC-Error ↑ μ Avg.	AUPRC-Error ↑ M Avg.	AUPRC-Success ↑ μ Avg.	AUPRC-Success ↑ M Avg.	FPR@95%TPR ↓ μ Avg.	FPR@95%TPR ↓ M Avg.
				DRN D-22			
Base	Var. Ratio	0.4383	0.4483	0.9950	0.9933	1.0000	0.4042
	Prob. Margin	0.4208	0.4308	0.9951	0.9934	1.0000	0.3716
	Entropy	0.4249	0.4316	0.9953	0.9936	0.2515	0.3104
Noise	Var. Ratio	0.4375	0.4483	0.9951	0.9933	1.0000	0.4037
	Prob. Margin	0.4198	0.4307	0.9951	0.9934	1.0000	0.3702
	Entropy	0.4246	0.4317	0.9953	0.9936	0.2515	0.3089
	Avg. Var.	0.3364	0.3320	0.9926	0.9912	1.0000	1.0000
	Max. Var.	0.3347	0.3300	0.9925	0.9912	1.0000	1.0000
	BALD	0.3231	0.3162	0.9892	0.9883	1.0000	0.9982
Scale	Var. Ratio	**0.4901**	**0.4850**	**0.9964**	**0.9954**	0.2134	0.2177
	Prob. Margin	0.4665	0.4624	**0.9964**	**0.9954**	0.2040	0.2070
	Entropy	0.4469	0.4402	0.9963	0.9952	**0.1988**	**0.1938**
	Avg. Var.	0.3167	0.3048	0.9946	0.9933	1.0000	0.6696
	Max. Var.	0.3153	0.2983	0.9946	0.9932	1.0000	0.6395
	BALD	0.3052	0.2940	0.9942	0.9931	0.2742	0.3224

				OneFormer ConvNeXt-L			
Base	Var. Ratio	0.1310	0.3090	0.9853	0.9633	0.8001	0.6999
	Prob. Margin	0.2300	0.3562	0.9885	0.9722	0.7587	0.5619
	Entropy	0.1193	0.2832	0.9847	0.9548	0.8034	0.7569
Noise	Var.Ratio	0.1356	0.3134	0.9849	0.9628	0.7973	0.6880
	Prob. Margin	0.2319	0.3590	0.9877	0.9691	0.7601	0.5556
	Entropy	0.1244	0.2886	0.9844	0.9540	0.7926	0.7674
	Avg. Var.	0.1255	0.2178	0.9913	0.9874	1.0000	0.9981
	Max. Var.	0.1141	0.2038	0.9909	0.9865	1.0000	0.9981
	BALD	0.1426	0.2335	0.9877	0.9858	1.0000	0.9981
Scale	Var. Ratio	0.1704	0.3258	0.9871	0.9741	0.7766	0.5904
	Prob. Margin	**0.2921**	**0.3808**	0.9905	0.9794	**0.7167**	**0.4413**
	Entropy	0.1424	0.2903	0.9860	0.9702	0.7961	0.6500
	Avg. Var.	0.1567	0.2303	**0.9931**	0.9886	1.0000	0.9970
	Max. Var.	0.1391	0.2101	0.9924	0.9883	1.0000	0.9971
	BALD	0.1916	0.2515	0.9928	**0.9897**	1.0000	0.9957
Drop	Var. Ratio	0.1454	0.3154	0.9855	0.9634	0.7865	0.6321
	Prob. Margin	0.2453	0.3614	0.9886	0.9703	0.7427	0.4868
	Entropy	0.1332	0.2888	0.9853	0.9537	0.7991	0.6994
	Avg. Var.	0.1480	0.2360	0.9921	0.9884	1.0000	0.9987
	Max. Var.	0.1353	0.2164	0.9916	0.9878	1.0000	0.9987
	BALD	0.1673	0.2557	0.9910	0.9890	1.0000	0.9987
				SegFormer B5			
Base	Var. Ratio	0.3873	0.4049	0.9969	0.9963	1.0000	0.7554
	Prob. Margin	0.3771	0.3935	0.9969	0.9963	1.0000	0.6954
	Entropy	0.3840	0.4038	0.9966	0.9961	1.0000	0.5757
Noise	Var. Ratio	0.3838	0.4021	0.9969	0.9964	1.0000	0.7575
	Prob. Margin	0.3724	0.3901	0.9969	0.9963	1.0000	0.6901
	Entropy	0.3826	0.4023	0.9967	0.9961	1.0000	0.5704
	Avg. Var.	0.3125	0.3210	0.9966	0.9962	1.0000	1.0000
	Max. Var.	0.3123	0.3204	0.9966	0.9962	1.0000	1.0000
	BALD	0.3073	0.3162	0.9915	0.9912	1.0000	1.0000
Scale	Var. Ratio	**0.4335**	**0.4422**	**0.9976**	**0.9971**	1.0000	0.3976
	Prob. Margin	0.4185	0.4256	**0.9976**	**0.9971**	1.0000	0.3642
	Entropy	0.4099	0.4233	0.9975	0.9965	1.0000	**0.2990**
	Avg. Var.	0.3371	0.3334	0.9975	**0.9971**	1.0000	0.9981
	Max. Var.	0.3352	0.3303	0.9975	**0.9971**	1.0000	0.9981
	BALD	0.3186	0.3155	0.9960	0.9955	1.0000	0.7832
Drop	Var. Ratio	0.3876	0.4051	0.9969	0.9963	1.0000	0.7481
	Prob. Margin	0.3770	0.3934	0.9968	0.9962	1.0000	0.6829
	Entropy	0.3843	0.4036	0.9966	0.9961	1.0000	0.5651
	Avg. Var.	0.3334	0.3425	0.9969	0.9965	1.0000	1.0000
	Max. Var.	0.3320	0.3410	0.9969	0.9965	1.0000	1.0000
	BALD	0.3211	0.3327	0.9917	0.9914	1.0000	0.9925

Finally, Table 13 and Table 14 show Precision and Recall for thresholding based on a maximum fraction of pixels allowed on Cityscapes and ADE20K datasets, respectively. We show results across three threshold values.

As expected, we see that as we increase the maximum number of pixels allowed, we get higher Recall at the cost of Precision. This observation holds true across all of the experiments. Again, we note that Scale often has the best performance with simple uncertainty metrics across both datasets.

Table 13: Micro and macro-averaged (μ and M, respectively) Precision and Recall for thresholding based on a maximum fraction of pixels allowed on the Cityscapes dataset.

Scene	Unc. Metric	Max 5% pixels Precision ↑ μ	M	Recall ↑ μ	M	Max 10% pixels Precision ↑ μ	M	Recall ↑ μ	M	Max 15% pixels Precision ↑ μ	M	Recall ↑ μ	M
						DRN D-22							
Base	VR	45.19	45.40	41.52	50.74	35.04	35.18	64.13	73.92	28.48	28.45	76.44	84.64
	PM	44.66	44.83	41.35	50.58	34.77	34.92	64.13	73.95	28.14	28.19	76.51	84.74
	E	44.04	44.23	39.76	48.74	34.80	35.03	63.64	73.61	28.11	28.23	76.42	84.73
Noise	VR	45.15	45.35	41.51	50.75	35.01	35.16	64.10	73.94	28.46	28.44	76.39	84.64
	PM	44.60	44.78	41.27	50.56	34.76	34.91	64.07	73.93	28.15	28.18	76.50	84.77
	E	44.02	44.20	39.75	48.77	34.79	35.02	63.64	73.64	28.12	28.23	76.45	84.78
	AV	40.06	39.93	32.11	38.45	38.03	37.47	50.03	55.62	37.92	36.97	55.23	58.76
	MV	39.79	39.66	31.88	38.17	37.81	37.22	49.85	55.45	37.65	36.70	55.34	58.86
	B	36.39	36.38	30.65	36.02	32.57	32.42	50.90	57.46	30.13	29.82	63.10	68.56
Scale	VR	**47.90**	**48.21**	43.77	52.63	36.67	36.94	67.41	76.23	29.11	29.28	79.80	**86.84**
	PM	47.17	47.44	43.46	52.41	36.33	36.59	67.23	76.08	28.92	29.10	**79.84**	86.82
	E	43.68	43.86	39.53	47.72	35.26	35.54	63.98	73.68	28.67	28.92	78.57	86.18
	AV	32.12	32.29	29.36	34.35	30.02	30.11	54.35	62.02	27.29	27.15	71.54	78.61
	MV	31.42	31.55	28.76	33.67	29.60	29.67	53.63	61.29	27.02	26.87	71.09	78.23
	B	31.13	31.32	28.39	32.45	28.38	28.55	51.55	57.83	25.34	25.41	68.24	74.57
						DRN D-105							
Base	VR	39.63	39.78	49.13	59.67	29.24	29.21	70.10	80.33	24.61	24.23	79.31	87.50
	PM	39.32	39.46	48.98	59.54	28.83	28.86	70.23	80.53	23.91	23.60	79.69	87.97
	E	39.72	39.95	48.70	59.33	28.85	28.94	70.48	80.80	23.15	22.99	80.26	88.63
Noise	VR	39.57	39.70	49.01	59.57	29.24	29.19	70.09	80.33	24.62	24.24	79.34	87.55
	PM	39.23	39.35	48.89	59.48	28.82	28.83	70.23	80.55	23.94	23.62	79.72	88.01
	E	39.66	39.90	48.58	59.24	28.83	28.92	70.51	80.82	23.17	23.00	80.32	88.67
	AV	40.51	40.32	40.62	48.14	39.37	38.74	50.96	56.09	39.41	38.64	52.14	56.53
	MV	40.36	40.17	40.64	48.16	39.28	38.64	51.00	56.08	39.34	38.55	52.17	56.51
	B	37.20	37.19	40.30	47.75	32.99	32.68	59.12	66.07	32.29	31.73	64.62	69.48
Scale	VR	**42.41**	**42.67**	52.51	62.94	30.32	30.47	74.36	83.62	23.97	23.82	84.09	91.08
	PM	42.07	42.31	52.42	62.88	30.07	30.23	74.33	83.65	23.48	23.45	**84.15**	91.18
	E	41.11	41.40	49.76	60.38	30.00	30.29	73.84	83.50	23.16	23.24	84.14	**91.32**
	AV.	35.74	35.87	43.55	51.63	30.48	30.24	68.84	77.10	28.21	27.52	79.36	84.93
	MV.	35.35	35.49	43.03	51.07	30.32	30.07	68.69	76.96	28.03	27.36	79.33	84.95
	B	33.45	33.64	40.73	47.25	27.51	27.57	65.47	73.22	23.51	23.33	79.31	85.81
						OneFormer ConvNeXt-L							
Base	VR	32.16	32.31	47.73	57.40	24.77	24.84	67.92	77.28	20.80	21.03	74.47	82.96
	PM	33.41	33.78	50.18	60.30	24.95	24.99	71.11	80.37	20.58	20.68	79.04	86.67
	E	30.89	31.47	44.48	54.09	23.82	24.11	64.18	74.15	20.07	20.51	70.79	79.86
Noise	VR	32.43	32.39	48.17	57.91	24.70	24.74	67.97	77.59	20.72	20.89	74.96	83.38
	PM	33.53	33.86	50.60	60.76	24.90	25.00	70.69	80.41	20.82	20.85	79.28	86.78
	E	31.29	31.41	45.12	54.88	24.19	24.24	65.25	74.79	20.46	20.73	71.70	80.37
	AV	28.32	30.65	23.29	27.49	25.39	29.84	27.17	30.78	24.23	29.78	28.87	32.20
	MV	26.90	29.38	21.05	24.74	23.40	28.55	24.70	27.96	22.19	28.49	26.33	29.30
	B	29.88	31.11	27.14	31.75	26.94	30.33	31.97	35.82	25.64	30.16	34.28	37.59
Scale	VR	33.06	33.12	49.59	59.05	24.31	24.37	70.19	79.48	20.03	20.18	77.58	85.63
	PM	**34.95**	**35.08**	53.07	62.79	24.83	24.94	73.38	82.40	20.01	20.04	**81.97**	**88.92**
	E	31.49	31.81	46.19	55.45	23.63	23.77	66.65	76.48	19.21	19.49	73.98	82.95
	AV	26.24	26.37	34.74	41.71	23.57	24.22	50.06	57.43	22.03	23.46	54.38	61.20

	MV	24.47	24.64	31.43	38.02	22.32	23.08	46.09	53.41	20.73	22.42	50.57	57.34
	B	27.69	27.71	38.17	45.61	24.49	24.68	55.98	63.55	22.87	23.67	60.90	67.73
Drop	VR	32.26	32.34	48.26	57.81	24.32	24.33	68.79	78.27	19.99	20.11	76.25	84.80
	PM	33.41	33.65	50.55	60.60	24.66	24.76	71.27	80.90	20.26	20.21	80.70	87.94
	E	31.03	31.47	45.20	54.88	23.63	23.72	65.94	75.90	19.41	19.59	72.95	82.24
	AV	27.22	28.30	29.97	37.42	25.57	27.51	39.85	47.02	24.53	27.53	41.76	48.59
	MV	25.91	26.88	27.07	33.79	24.04	26.38	35.73	42.43	23.02	26.34	37.48	43.91
	B	28.84	29.05	34.44	42.68	26.69	27.84	46.91	54.52	25.52	27.71	49.72	56.72
						OneFormer Swin-L							
Base	VR	32.94	33.23	49.05	57.91	24.85	24.96	69.57	77.97	20.84	20.77	78.74	84.70
	PM	34.55	34.74	51.98	61.02	25.30	25.40	72.51	80.80	20.86	20.73	81.77	87.42
	E	31.81	32.27	45.96	54.81	24.24	24.56	66.79	75.25	20.25	20.52	75.56	81.89
Noise	VR	33.11	33.47	49.38	58.24	24.97	25.05	70.12	78.27	20.99	20.94	79.10	84.90
	PM	34.73	34.88	52.24	61.27	25.36	25.39	72.93	80.98	20.70	20.58	81.90	87.55
	E	32.04	32.58	46.64	55.36	24.33	24.57	67.07	75.50	20.33	20.55	76.08	82.28
	AV	29.87	31.00	26.77	30.33	27.68	30.23	31.40	34.14	26.58	30.07	32.79	35.08
	MV	28.28	29.58	24.38	27.57	26.22	28.98	28.79	31.26	25.39	28.89	30.04	32.11
	B	31.24	31.81	30.48	34.60	28.89	30.78	36.27	39.23	27.91	30.66	38.01	40.31
Scale	VR	33.94	34.32	50.84	59.78	25.02	25.08	73.38	80.83	20.08	19.99	82.28	87.82
	PM	**35.94**	**36.36**	54.53	63.51	25.64	25.65	76.29	83.36	19.98	19.84	**84.67**	**90.01**
	E	32.44	32.95	47.77	56.50	24.29	24.38	70.42	78.41	19.44	19.53	79.54	85.80
	AV	27.75	27.90	37.81	44.46	24.89	25.01	57.01	62.72	23.77	24.16	63.79	67.53
	MV	25.97	26.06	34.85	40.95	23.92	24.09	53.77	59.28	22.74	23.24	60.39	64.22
	B	29.08	29.14	41.04	47.95	25.57	25.34	61.88	67.78	24.06	24.11	69.03	72.82
Drop	VR	32.99	33.47	49.35	58.22	24.84	24.91	70.67	78.76	20.58	20.55	79.87	85.54
	PM	34.51	34.86	52.25	61.35	25.26	25.31	73.34	81.33	20.42	20.32	82.53	88.16
	E	31.84	32.43	46.51	55.32	23.95	24.13	67.69	76.26	19.89	19.97	77.17	83.17
	AV	29.79	30.33	33.67	40.77	27.84	29.11	43.91	50.12	26.93	28.82	46.11	51.68
	MV	28.13	28.72	30.60	37.09	26.50	27.96	40.00	45.77	25.88	27.83	41.88	47.13
	B	31.21	31.36	38.42	46.14	28.73	29.50	50.96	57.41	27.71	29.06	53.38	59.08
						SegFormer B5							
Base	VR	36.62	36.67	54.75	63.87	27.19	26.95	74.08	81.94	24.94	24.49	80.02	86.05
	PM	36.39	36.44	54.79	63.96	26.68	26.48	74.42	82.37	23.88	23.45	81.16	87.19
	E	36.61	36.71	54.78	63.98	26.09	25.99	74.94	83.01	22.42	22.02	82.52	88.66
Noise	VR	36.50	36.54	54.61	63.79	27.16	26.91	74.01	81.90	24.87	24.42	80.04	86.09
	PM	36.29	36.34	54.60	63.82	26.65	26.45	74.41	82.36	23.82	23.39	81.15	87.21
	E	36.49	36.60	54.55	63.83	26.04	25.94	74.84	82.98	22.36	21.96	82.56	88.71
	AV	**40.42**	**40.39**	38.53	43.44	40.25	40.13	41.31	45.00	40.19	40.11	41.61	45.11
	MV	**40.42**	40.36	38.38	43.21	40.19	40.07	41.25	44.84	40.18	40.07	41.46	44.90
	B	35.96	36.06	42.17	48.35	34.23	34.20	52.27	56.64	34.07	34.05	53.50	57.22
Scale	VR	38.52	38.66	57.84	66.40	27.03	26.98	78.45	85.47	22.33	21.92	86.20	91.23
	PM	38.36	38.49	57.89	66.44	26.68	26.68	78.68	85.68	21.55	21.23	86.60	91.67
	E	37.88	38.15	56.12	65.23	26.49	26.57	78.44	85.68	20.75	20.54	**86.91**	**92.12**
	AV	34.28	34.28	49.87	57.04	29.54	29.07	72.25	78.02	28.45	27.81	77.68	81.50
	MV	34.09	34.09	49.70	56.83	29.38	28.91	72.37	78.12	28.26	27.62	77.88	81.69
	B	31.46	31.51	46.09	52.15	25.41	25.31	71.04	77.64	22.48	22.11	81.72	86.61
Drop	VR	36.62	36.67	54.79	63.92	27.17	26.93	74.15	82.01	24.81	24.35	80.25	86.25
	PM	36.42	36.47	54.80	63.96	26.64	26.45	74.51	82.45	23.76	23.33	81.35	87.36
	E	36.61	36.73	54.74	63.96	26.05	25.96	74.96	83.06	22.31	21.92	82.68	88.80
	AV	38.44	38.37	47.21	54.70	37.02	36.69	56.13	61.53	37.02	36.66	56.64	61.71
	MV	38.39	38.33	46.98	54.43	37.06	36.72	55.80	61.20	37.06	36.69	56.31	61.38
	B	34.73	34.82	45.35	52.84	29.60	29.53	65.38	72.44	28.96	28.77	69.43	75.02

Table 14: Micro and macro-averaged (μ and M, respectively) Precision and Recall for thresholding based on a maximum fraction of pixels allowed on the ADE20K dataset.

Scene	Unc. Metric	Max 5% pixels Precision ↑ μ	M	Recall ↑ μ	M	Max 10% pixels Precision ↑ μ	M	Recall ↑ μ	M	Max 15% pixels Precision ↑ μ	M	Recall ↑ μ	M
						OneFormer ConvNeXt-L							
Base	VR	47.06	48.64	13.71	26.63	41.24	42.80	22.95	39.37	37.98	39.10	30.06	47.02
	PM	50.10	52.72	13.67	27.27	44.99	47.46	24.82	42.06	41.45	43.45	34.19	51.95
	E	43.42	45.63	11.38	23.14	38.09	40.24	19.18	34.30	34.36	36.72	24.40	40.23
Noise	VR	46.82	48.40	13.60	26.50	40.80	42.62	22.69	39.25	37.48	38.92	29.51	46.74
	PM	49.72	51.84	13.56	26.82	44.48	46.83	24.65	41.97	41.35	43.13	34.27	51.96
	E	43.29	45.73	11.36	23.11	37.44	39.87	18.91	34.23	34.22	36.50	24.11	40.07
	AV	35.66	37.79	08.32	14.39	34.12	36.78	14.30	21.51	32.70	36.13	18.94	26.12
	MV	34.75	37.29	07.96	13.66	33.20	36.16	13.66	20.13	31.75	35.70	17.86	24.32
	B	37.41	37.75	09.20	14.77	34.55	35.70	16.07	23.16	33.63	34.57	22.48	29.42
Scale	VR	48.64	50.01	14.37	27.55	41.80	43.48	23.98	40.57	38.22	39.40	31.20	48.36
	PM	**51.85**	**54.22**	14.63	28.57	45.91	48.29	26.21	43.75	41.99	44.14	**35.70**	**53.54**
	E	44.02	46.12	11.83	23.81	37.77	39.70	19.77	35.24	34.16	35.94	25.65	41.55
	AV	33.02	33.00	08.90	15.87	31.13	32.04	16.00	25.62	30.02	31.46	22.35	32.39
	MV	31.15	31.46	08.22	14.56	29.56	30.60	14.87	23.66	28.26	30.01	20.47	29.77
	B	37.05	37.00	10.57	18.79	34.67	34.90	19.06	30.30	32.94	33.54	26.15	38.40
Drop	VR	47.23	48.70	13.88	26.96	41.36	42.79	23.23	39.93	37.82	38.97	30.23	47.41
	PM	50.62	52.55	14.06	27.53	45.01	47.40	25.44	42.56	41.51	43.43	34.83	52.39
	E	43.48	45.72	11.61	23.58	37.55	39.90	19.32	34.64	34.41	36.36	25.01	40.94
	AV	32.91	34.23	08.39	15.68	31.96	33.95	15.30	24.70	30.97	33.53	21.32	31.35
	MV	31.38	33.16	07.89	14.49	30.31	32.86	14.19	22.54	29.59	32.70	19.63	28.57
	B	35.57	36.53	09.66	18.33	34.25	35.34	18.07	29.48	33.37	34.64	25.62	38.02
						OneFormer Swin-L							
Base	VR	46.97	48.39	14.18	27.16	41.28	42.31	23.92	40.21	38.27	38.78	31.45	47.94
	PM	49.35	51.85	14.19	27.81	44.07	46.13	25.34	42.57	41.18	42.29	35.43	52.68
	E	43.36	45.43	11.87	23.72	37.71	39.28	20.01	34.95	34.84	35.71	26.00	41.07
Noise	VR	46.76	48.02	14.18	26.98	41.26	42.21	24.00	40.25	38.13	38.55	31.40	47.83
	PM	49.39	51.30	14.30	27.85	44.03	45.67	25.47	42.60	40.67	41.89	35.15	52.55
	E	42.99	45.13	11.89	23.66	37.56	39.34	19.86	34.81	34.67	35.65	26.07	41.10
	AV	33.66	35.65	08.40	14.71	32.44	35.30	14.46	22.00	30.69	34.96	19.15	27.13
	MV	32.74	34.93	07.97	13.72	31.41	34.61	13.67	20.48	29.65	34.08	18.00	25.09
	B	36.48	37.19	09.60	16.23	33.93	35.36	17.18	25.26	32.10	34.11	23.16	31.76
Scale	VR	48.38	49.56	14.85	28.10	41.74	42.90	25.00	41.66	38.39	39.05	32.99	49.81
	PM	**51.02**	**52.71**	15.09	28.78	45.13	46.90	27.08	44.40	41.36	42.87	**36.75**	**54.48**
	E	43.48	45.43	12.25	24.32	37.57	39.17	20.63	35.87	34.33	35.33	26.97	42.45
	AV	34.14	34.12	09.65	17.18	32.33	32.78	17.57	27.72	30.42	31.87	23.84	34.88
	MV	32.14	32.40	08.90	15.81	30.23	31.10	16.14	25.39	28.56	30.32	21.88	31.85
	B	37.85	37.71	11.38	20.03	35.90	35.87	20.74	32.48	33.65	34.27	28.15	41.15
Drop	VR	47.08	48.53	14.39	27.37	41.44	42.34	24.48	40.77	38.36	38.68	31.94	48.42
	PM	50.04	52.30	14.62	28.21	44.52	46.35	26.12	43.17	41.48	42.47	36.28	53.25
	E	43.07	45.14	12.06	23.97	37.85	39.12	20.53	35.48	34.68	35.35	26.65	41.70
	AV	32.02	33.24	08.56	15.45	30.49	32.83	15.41	24.45	29.64	32.45	21.13	30.64
	MV	30.58	31.90	07.99	14.26	29.13	31.69	14.23	22.27	28.17	31.49	19.49	27.95
	B	34.35	35.55	09.68	17.86	33.17	34.43	18.12	29.11	32.11	33.38	25.36	37.35
						SegFormer B5							
Base	VR	55.19	55.90	16.38	29.25	48.88	49.68	29.08	46.12	44.74	45.38	39.35	57.38

	PM	53.48	54.15	15.97	28.81	48.18	48.93	28.83	45.86	44.27	44.92	39.22	57.25
	E	54.69	55.50	16.07	28.51	48.63	49.74	28.67	45.76	44.33	45.40	39.16	57.46
Noise	VR	55.21	55.90	16.39	29.24	48.90	49.68	29.10	46.14	44.73	45.37	39.34	57.38
	PM	53.50	54.13	15.97	28.81	48.19	48.93	28.82	45.87	44.26	44.89	39.19	57.25
	E	54.61	55.45	16.02	28.48	48.60	49.71	28.66	45.74	44.29	45.35	39.13	57.45
	AV	49.94	50.55	13.87	24.11	48.42	48.36	24.92	38.74	47.80	47.03	33.24	47.63
	MV	49.83	50.43	13.79	23.94	48.28	48.24	24.78	38.57	47.61	46.92	33.19	47.52
	B	48.63	49.49	13.84	23.18	45.82	46.51	25.20	38.80	44.00	44.23	34.62	49.73
Scale	VR	**57.22**	**58.41**	16.86	29.97	50.55	51.87	30.04	47.26	45.83	47.10	**40.67**	**58.91**
	PM	54.98	56.10	16.23	29.29	49.43	50.66	29.52	46.70	45.15	46.38	40.34	58.50
	E	55.19	56.35	16.16	28.46	49.43	50.91	29.07	46.08	45.05	46.61	39.71	58.12
	AV	44.61	46.20	13.17	22.04	43.34	44.56	25.23	38.40	42.16	42.98	35.75	50.37
	MV	44.17	45.76	13.04	21.84	42.86	44.17	24.99	38.12	41.82	42.68	35.53	50.13
	B	45.28	47.00	13.38	21.49	42.71	44.29	25.22	37.42	40.59	41.95	35.64	49.61
Drop	VR	55.26	55.97	16.40	29.26	48.92	49.72	29.12	46.18	44.71	45.40	39.38	57.45
	PM	53.53	54.18	15.98	28.81	48.20	48.95	28.85	45.89	44.27	44.93	39.23	57.30
	E	54.62	55.46	16.06	28.46	48.65	49.78	28.68	45.75	44.32	45.42	39.14	57.47
	AV	51.84	52.71	15.04	26.50	48.66	49.12	27.29	43.02	46.72	46.54	37.01	53.72
	MV	51.47	52.41	14.92	26.34	48.43	48.90	27.09	42.82	46.49	46.39	36.88	53.62
	B	51.86	52.96	15.10	25.75	47.11	48.29	27.14	42.33	43.76	44.77	37.09	53.92

Considering all these results, we would suggest using either Base or Scale to gauge the trustworthiness of a network. Base is computationally much cheaper, but Scale generally provides better results. As for the uncertainty metric, it is best to use the simpler metrics like Variation Ratio, Probability Margin and Entropy since they seem to provide the best results in most cases. It also seems that for in-domain data, thresholding based on a maximum fraction of pixels is better than using the largest difference.

B Dark Zurich

We now provide all results on the Dark Zurich dataset. Since Dark Zurich was used to test how well the metrics work when there is a shift in the input domain, all networks perform poorly on the dataset. Table 15 shows the base performance of the models on the dataset.

DRN performs very poorly, while OneFormer and SegFormer provide much more respectable results. Overall, the results are quite poor and show that, in general, these networks do not handle large changes in input domain well.

Table 15: Micro and macro-averaged (μ and M, respectively) Mean Intersection Over Union (mIoU), Expected Calibration Error (ECE) and Brier Score (BS) on the Dark Zurich dataset.

Model	mIoU ↑		ECE ↓		BS ↓	
	μ Avg.	M Avg.	μ Avg.	M Avg.	μ Avg.	M Avg.
DRN D-22	0.0710	0.0737	0.3067	0.5142	1.1303	1.1361
DRN D-105	0.0951	0.0990	0.2877	0.4173	0.9259	0.9315
OneFormer ConvNeXt-L	**0.3994**	0.3752	0.5964	0.5755	0.8340	0.8345
OneFormer Swin-L	**0.3994**	**0.3949**	0.5988	0.6678	0.8259	0.8263
SegFormer B5	0.3128	0.2686	**0.2212**	**0.2715**	**0.6053**	**0.6063**

Table 16 shows the AUROC and the performance of thresholding based on the largest difference, and Table 17 shows the results when we use a maximum fraction of pixels as the thresholding metric.

Even with such poor performance, we observe that the largest difference thresholding is able to achieve AUROC of 0.7 or greater. Precision suffers a bit in this scenario, but Recall is excellent, and while a large fraction of pixels are selected, it is often correct since most pixels are actually misclassified. Scale with Probability Margin as the uncertainty metric often performs the best, similar to earlier experiments.

On the other hand, thresholding based on a maximum fraction of pixels is less useful in this case, with Recall being much lower than the largest difference method. This is because, as explained earlier, most pixels are actually misclassified and restricting it to a maximum of 15% actually hurts performance.

Table 16: Micro and macro-averaged (μ and M, respectively) Area Under Receiver Operating Characteristic (AUROC) and Precision, Recall and the fraction of pixels selected for largest difference thresholding on the Dark Zurich dataset.

Scenario	Uncertainty Metric	AUROC ↑		Largest Difference Thresholding					
				Precision ↑		Recall ↑		Pixel %	
		μ Avg.	M Avg.	μ Avg.	M Avg.	μ Avg.	M Avg.	μ Avg.	M Avg.
				DRN D-22					
Base	Var. Ratio	0.6060	0.6061	70.14	70.63	74.73	75.07	70.05	70.01
	Prob. Margin	0.6056	0.6067	69.67	70.18	77.53	77.85	73.16	73.11
	Entropy	0.6054	0.6062	68.92	69.46	80.93	81.24	77.21	77.15
Noise	Var. Ratio	0.6027	0.6038	69.96	70.49	74.81	75.17	70.31	70.26
	Prob. Margin	0.6021	0.6041	69.50	70.05	77.57	77.91	73.39	73.33
	Entropy	0.6024	0.6038	68.77	69.35	80.95	81.28	77.39	77.32
	Avg. Var.	0.5892	0.5918	**75.12**	**75.56**	46.70	46.99	40.87	40.89
	Max. Var.	0.5898	0.5922	75.04	75.47	47.31	47.60	41.46	41.47
	BALD	0.6113	0.6185	73.39	74.13	63.25	63.62	56.66	56.62
Scale	Var. Ratio	0.6835	0.6853	69.46	70.14	94.25	94.42	89.22	89.21
	Prob. Margin	**0.6849**	**0.6864**	68.47	69.26	**95.12**	**95.40**	91.34	91.31
	Entropy	0.6680	0.6714	71.92	72.34	79.24	79.24	72.45	72.67
	Avg. Var.	0.6769	0.6771	71.45	71.78	91.80	91.93	84.48	84.48
	Max. Var.	0.6763	0.6766	71.16	71.51	92.49	92.61	85.46	85.46
	BALD	0.6808	0.6809	69.02	69.77	93.96	94.32	89.51	89.41
				DRN D-105					
Base	Var. Ratio	0.6909	0.6722	65.35	64.55	77.75	77.90	64.00	64.30
	Prob. Margin	0.6944	0.6749	64.45	63.68	80.71	80.82	67.35	67.66
	Entropy	0.6954	0.6756	63.41	62.68	83.74	83.88	71.03	71.35
Noise	Var. Ratio	0.6951	0.6765	65.42	64.54	78.16	78.25	64.26	64.55
	Prob. Margin	0.6986	0.6793	64.50	63.65	81.08	81.13	67.61	67.91
	Entropy	0.6994	0.6795	63.44	62.66	84.12	84.18	71.31	71.62
	Avg. Var.	0.6597	0.6499	**72.46**	**71.56**	53.21	53.57	39.50	39.70
	Max. Var.	0.6594	0.6496	72.30	71.41	53.50	53.90	39.80	40.00
	BALD	0.6951	0.6820	68.93	68.17	69.57	69.91	54.28	54.56
Scale	Var. Ratio	0.7514	0.7291	61.32	60.82	91.13	91.52	79.94	80.29
	Prob. Margin	**0.7520**	**0.7295**	60.48	60.08	**91.99**	**92.49**	81.80	82.15
	Entropy	0.7410	0.7184	59.96	60.21	88.06	89.04	78.99	79.12
	Avg. Var.	0.7369	0.7168	65.89	64.95	83.86	83.77	68.46	68.80
	Max. Var.	0.7368	0.7149	65.51	64.57	84.64	84.53	69.49	69.83
	BALD	0.7433	0.7225	62.10	61.33	90.92	90.90	78.75	79.09
				OneFormer ConvNeXt-L					
Base	Var. Ratio	0.5855	0.6168	38.21	39.15	60.89	64.90	46.06	46.13
	Prob. Margin	0.6221	0.6604	40.17	41.14	66.90	70.26	48.14	48.38
	Entropy	0.5667	0.5949	38.41	39.55	56.71	60.16	42.67	42.79
Noise	Var. Ratio	0.5810	0.6297	41.12	41.79	62.40	64.63	43.86	44.11
	Prob. Margin	0.6235	0.6731	44.26	44.16	70.58	71.58	46.09	46.43
	Entropy	0.5641	0.6036	41.33	42.15	56.58	58.65	39.57	39.84

	Avg. Var.	0.6185	0.5884	45.33	43.47	49.41	46.04	31.51	31.94
	Max. Var.	0.6061	0.5770	44.69	42.99	46.14	42.97	29.84	30.22
	BALD	0.6408	0.6098	46.09	44.01	54.68	51.24	34.29	34.82
Scale	Var. Ratio	0.6645	0.7152	42.57	43.90	77.82	80.84	52.83	52.83
	Prob. Margin	0.7136	0.7483	42.30	42.50	**86.97**	**88.44**	59.42	59.58
	Entropy	0.6377	0.7012	42.47	43.69	73.21	77.11	49.82	49.79
	Avg. Var.	0.7535	0.7529	47.01	47.51	79.58	79.77	48.93	49.27
	Max. Var.	0.7375	0.7389	**46.93**	47.73	75.94	76.41	46.78	47.11
	BALD	**0.7782**	**0.7702**	46.55	**48.37**	84.16	83.93	52.26	52.63
Drop	Var. Ratio	0.5911	0.6229	38.94	39.56	62.37	65.38	46.30	46.49
	Prob. Margin	0.6249	0.6608	40.57	41.36	70.08	73.29	49.93	50.09
	Entropy	0.5755	0.6089	39.10	40.23	57.44	61.24	42.46	42.61
	Avg. Var.	0.6007	0.5568	41.51	42.21	50.29	46.64	35.02	35.36
	Max. Var.	0.5884	0.5424	39.94	40.71	47.21	42.98	34.16	34.50
	BALD	0.6246	0.5831	43.23	43.76	61.41	57.44	41.06	41.61
					OneFormer Swin-L				
Base	Var. Ratio	0.6779	0.7245	30.32	31.88	76.77	79.86	51.50	51.69
	Prob. Margin	0.7280	0.7592	30.33	31.68	82.61	85.43	55.40	55.62
	Entropy	0.6555	0.7020	30.87	31.99	72.48	75.92	47.75	48.00
Noise	Var. Ratio	0.6483	0.6946	29.73	31.70	75.11	78.96	51.38	51.44
	Prob. Margin	0.6926	0.7253	30.44	31.83	82.02	84.50	54.80	54.92
	Entropy	0.6293	0.6770	29.85	31.36	70.65	74.42	48.13	48.15
	Avg. Var.	0.6410	0.6416	33.52	35.01	56.22	56.33	34.11	34.37
	Max. Var.	0.6307	0.6288	33.44	35.05	53.37	53.36	32.46	32.70
	BALD	0.6670	0.6635	**34.19**	35.52	63.24	62.72	37.62	37.98
Scale	Var. Ratio	0.7211	0.7414	29.35	30.90	87.33	89.37	60.52	60.78
	Prob. Margin	**0.7577**	**0.7662**	30.10	31.51	**93.48**	**94.12**	63.17	63.49
	Entropy	0.7008	0.7259	29.76	31.32	80.13	82.50	54.77	54.87
	Avg. Var.	0.6925	0.6958	29.62	31.29	82.56	83.32	56.69	57.03
	Max. Var.	0.6752	0.6806	29.78	31.03	78.57	79.66	53.65	53.92
	BALD	0.7250	0.7221	30.32	31.52	85.74	86.40	57.50	57.76
Drop	Var. Ratio	0.6956	0.7290	29.63	31.56	79.85	83.26	54.81	54.88
	Prob. Margin	0.7379	0.7591	29.56	31.19	86.79	88.97	59.71	59.94
	Entropy	0.6736	0.7098	30.07	31.84	74.97	78.39	50.70	50.75
	Avg. Var.	0.6046	0.6040	31.75	35.61	49.89	50.91	31.95	31.96
	Max. Var.	0.5834	0.5822	30.39	34.46	44.06	45.19	29.49	29.42
	BALD	0.6471	0.6387	33.59	**36.63**	59.41	59.76	35.97	36.06
					SegFormer B5				
Base	Var. Ratio	0.7999	0.7978	61.71	60.47	83.55	83.24	48.95	49.18
	Prob. Margin	0.8053	0.8033	60.56	59.34	85.81	85.53	51.23	51.46
	Entropy	0.8155	0.8156	58.55	57.43	89.42	89.24	55.22	55.47
Noise	Var. Ratio	0.7949	0.7903	62.18	60.54	82.73	82.46	48.10	48.26
	Prob. Margin	0.8012	0.7966	61.02	59.40	85.26	84.98	50.52	50.69
	Entropy	0.8130	0.8092	58.85	57.44	89.09	88.89	54.74	54.93
	Avg. Var.	0.6740	0.6721	67.72	67.33	47.74	47.73	25.48	25.56
	Max. Var.	0.6743	0.6724	67.80	67.37	47.72	47.71	25.45	25.51
	BALD	0.7243	0.7217	65.13	64.02	63.62	63.44	35.31	35.39
Scale	Var. Ratio	0.8474	0.8490	56.87	55.85	94.71	94.56	60.21	60.54
	Prob. Margin	0.8483	0.8491	55.76	54.76	95.73	95.62	62.06	62.38
	Entropy	**0.8519**	**0.8566**	53.81	52.90	**97.22**	**97.22**	65.32	65.63
	Avg. Var.	0.8064	0.8045	62.63	61.51	84.98	84.79	49.06	49.35
	Max. Var.	0.8088	0.8060	62.39	61.25	85.59	85.37	49.60	49.90
	BALD	0.8247	0.8249	57.76	56.68	93.09	92.86	58.27	58.59

Drop	Var. Ratio	0.8013	0.7990	61.58	60.33	83.92	83.58	49.27	49.50
	Prob. Margin	0.8065	0.8043	60.42	59.19	86.15	85.83	51.55	51.78
	Entropy	0.8165	0.8163	58.37	57.24	89.68	89.48	55.55	55.80
	Avg. Var.	0.6980	0.6990	69.68	68.43	51.47	51.90	26.70	26.78
	Max. Var.	0.6979	0.6976	**70.03**	**68.67**	51.20	51.42	26.43	26.50
	BALD	0.7539	0.7532	65.18	64.02	69.57	69.40	38.59	38.75

Table 17: Micro and macro-averaged (μ and M, respectively) Precision and Recall for thresholding based on a maximum fraction of pixels allowed on the Dark Zurich dataset.

Scene	Unc. Metric	Max 5% pixels				Max 10% pixels				Max 15% pixels			
		Precision ↑		Recall ↑		Precision ↑		Recall ↑		Precision ↑		Recall ↑	
		μ	M	μ	M	μ	M	μ	M	μ	M	μ	M
						DRN D-22							
Base	VR	80.81	80.86	05.86	05.94	79.04	79.14	11.65	11.79	77.96	78.11	17.41	17.61
	PM	78.91	79.08	05.74	05.81	78.24	78.41	11.63	11.76	77.62	77.77	17.41	17.59
	E	81.07	81.12	05.92	06.01	78.88	78.96	11.57	11.74	77.51	77.58	17.03	17.23
Noise	VR	79.99	80.04	05.75	05.83	78.31	78.44	11.49	11.63	77.40	77.56	17.24	17.43
	PM	77.93	78.09	05.63	05.69	77.36	77.56	11.45	11.58	76.98	77.16	17.27	17.45
	E	80.71	80.78	05.92	06.01	78.48	78.56	11.59	11.74	77.12	77.22	16.98	17.19
	AV	77.78	77.89	05.65	05.69	77.46	77.62	11.13	11.20	77.28	77.46	16.58	16.68
	MV	77.75	77.81	05.64	05.68	77.27	77.53	11.18	11.25	77.17	77.43	16.57	16.69
	B	77.99	78.09	05.65	05.70	77.99	78.30	11.22	11.32	77.93	78.23	16.78	16.92
Scale	VR	83.99	84.07	06.03	06.13	82.50	82.54	11.97	12.16	81.54	81.62	17.83	18.10
	PM	82.04	82.13	05.49	05.56	81.63	81.73	11.75	11.92	81.09	81.22	**17.87**	**18.13**
	E	**84.60**	**84.61**	06.08	06.18	81.69	81.80	11.88	12.08	80.24	80.34	17.67	17.94
	AV	76.09	76.20	05.45	05.50	76.80	76.91	11.22	11.33	77.37	77.53	16.96	17.13
	MV	75.39	75.64	05.48	05.52	76.65	76.87	11.27	11.37	77.42	77.68	17.04	17.21
	B	81.40	81.51	05.87	05.94	79.81	79.95	11.60	11.73	79.19	79.32	17.43	17.61
						DRN D-105							
Base	VR	79.49	79.57	06.99	07.54	77.15	77.21	13.95	14.92	75.53	75.57	20.69	21.99
	PM	78.21	78.21	07.00	07.49	76.79	76.80	14.02	14.95	75.38	75.42	20.73	22.02
	E	78.96	79.07	07.03	07.59	76.02	76.04	13.50	14.44	74.43	74.49	19.73	21.04
Noise	VR	79.45	79.67	07.01	07.55	77.69	77.87	14.08	15.07	76.24	76.40	20.83	22.21
	PM	78.74	78.86	07.01	07.54	77.46	77.60	14.10	15.06	76.13	76.30	20.91	22.28
	E	78.57	78.76	06.98	07.54	76.16	76.30	13.49	14.45	74.78	74.96	19.91	21.27
	AV	82.54	82.55	07.32	07.80	80.39	80.35	14.29	15.18	78.53	78.51	20.94	22.18
	MV	82.35	82.37	07.34	07.82	80.21	80.12	14.26	15.14	78.36	78.36	20.82	22.01
	B	83.58	83.48	07.41	07.91	81.03	81.08	14.36	15.31	79.27	79.24	21.10	22.38
Scale	VR	**85.07**	**85.04**	07.44	08.09	83.39	83.39	14.81	15.95	81.64	81.69	21.89	23.48
	PM	83.96	83.95	07.22	07.84	82.98	82.98	14.79	15.93	81.75	81.75	**22.28**	**23.85**
	E	81.47	81.53	07.09	07.70	78.75	78.91	13.96	15.06	76.88	77.00	20.53	21.96
	AV	80.17	80.07	07.04	07.52	79.30	79.18	14.21	15.06	78.35	78.17	21.11	22.31
	MV	79.46	79.40	07.02	07.49	78.23	78.17	14.07	14.93	77.44	77.35	20.89	22.10
	B	83.78	83.56	07.35	07.95	81.43	81.31	14.51	15.53	79.77	79.67	21.41	22.75
						OneFormer ConvNeXt-L							
Base	VR	55.89	55.76	08.77	09.96	50.95	51.16	16.68	18.75	49.33	49.48	24.12	27.14
	PM	56.90	57.26	08.92	10.33	52.74	52.69	17.00	19.15	50.50	50.72	25.34	28.66
	E	53.66	57.98	07.10	07.95	50.51	52.77	15.43	17.23	48.45	48.76	23.19	26.27
Noise	VR	50.88	50.21	08.01	09.27	48.60	48.81	15.88	18.17	48.02	48.27	23.52	26.45

	PM	53.23	53.87	08.42	09.64	51.40	51.91	16.85	19.14	51.08	51.35	25.31	28.26
	E	49.02	51.82	06.52	07.39	49.29	48.66	15.02	17.19	48.25	48.43	22.81	25.61
	AV	46.85	45.04	06.36	07.00	44.08	43.39	12.61	13.80	43.62	43.65	17.48	19.20
	MV	45.42	43.87	06.00	06.62	43.74	42.74	11.67	12.69	42.86	42.59	16.37	17.96
	B	48.90	47.01	07.34	08.14	46.53	45.87	13.75	15.10	46.43	46.20	20.19	22.12
Scale	VR	52.04	51.60	07.88	08.93	48.94	49.20	15.42	17.39	50.30	50.41	24.27	27.58
	PM	46.41	47.38	06.59	07.49	48.77	48.99	15.34	17.39	50.86	50.86	24.99	28.57
	E	51.66	50.42	06.92	08.08	51.24	51.17	14.99	17.19	51.33	51.43	23.35	26.61
	AV	52.01	51.73	07.79	08.84	56.87	55.85	16.98	19.21	57.48	56.90	25.91	29.41
	MV	51.34	49.82	06.96	07.83	55.74	53.54	14.94	17.66	57.64	55.91	24.48	28.40
	B	**57.51**	**57.99**	09.13	10.25	58.43	58.94	18.77	21.02	58.65	59.66	**28.41**	**31.66**
Drop	VR	51.98	51.69	08.09	09.25	49.13	49.10	16.15	18.31	48.15	48.37	23.93	26.97
	PM	51.11	51.05	07.99	09.14	49.69	49.70	16.39	18.56	49.00	49.12	24.54	27.56
	E	52.52	50.47	06.85	07.76	50.17	48.08	15.28	17.34	47.78	47.82	22.84	25.84
	AV	38.57	37.21	04.57	05.25	39.58	38.91	09.37	10.53	37.29	36.68	13.84	15.12
	MV	38.98	36.21	04.45	05.15	37.04	34.95	08.49	09.52	36.13	35.49	13.12	14.32
	B	39.47	38.96	04.86	05.60	39.04	40.32	10.22	11.43	39.46	39.81	15.44	17.16
						OneFormer Swin-L							
Base	VR	56.31	57.18	12.60	13.72	52.36	52.90	24.12	26.45	48.69	49.42	33.07	36.21
	PM	**56.72**	**57.57**	11.37	13.35	55.15	55.24	25.23	28.12	51.94	52.22	**36.61**	**40.07**
	E	52.69	55.74	09.64	11.01	50.94	53.44	21.54	23.85	47.18	49.77	29.67	32.64
Noise	VR	47.88	49.03	10.66	11.51	45.92	46.34	21.15	22.78	42.87	43.36	29.80	31.88
	PM	47.28	49.55	10.06	11.08	46.03	46.35	21.56	23.40	44.13	44.37	31.53	33.76
	E	47.89	50.21	09.52	10.16	45.17	47.59	19.38	21.13	42.15	42.67	28.22	30.05
	AV	40.68	39.68	08.21	08.92	37.55	38.22	15.33	16.84	37.95	38.76	22.46	24.85
	MV	37.52	38.19	07.38	08.13	37.55	38.72	14.63	16.60	35.51	36.92	21.04	23.13
	B	42.65	42.53	09.14	09.80	41.62	41.63	17.70	19.21	39.95	40.22	25.51	27.80
Scale	VR	48.65	49.65	10.46	11.12	46.42	47.06	20.92	22.38	45.17	45.57	31.19	33.47
	PM	43.23	46.15	08.91	09.53	44.32	44.66	20.25	21.83	45.21	45.28	31.92	34.26
	E	46.59	48.57	09.34	10.13	46.59	48.38	19.30	21.02	44.81	45.35	29.41	31.71
	AV	36.17	35.70	08.00	08.83	36.06	35.52	16.22	17.54	36.04	36.23	24.61	26.69
	MV	33.22	32.79	07.13	08.06	34.45	33.58	14.99	16.49	35.30	34.60	23.07	25.30
	B	42.63	42.15	09.55	09.89	41.67	41.58	19.41	20.26	40.87	41.04	28.37	29.89
Drop	VR	53.68	54.48	11.89	12.78	50.24	50.64	23.10	25.08	47.42	47.96	33.15	35.84
	PM	50.47	51.85	10.43	11.89	51.13	51.63	23.81	26.40	49.95	50.33	35.11	38.40
	E	52.31	56.24	09.76	10.67	49.54	52.10	21.05	23.13	46.24	48.85	30.17	33.00
	AV.	32.22	36.01	05.65	06.56	35.33	37.06	12.58	14.02	33.60	35.12	16.58	18.30
	MV.	31.64	35.13	05.12	05.95	32.18	33.85	10.85	12.03	30.54	32.84	15.57	17.30
	B	36.19	37.58	07.08	08.17	38.70	40.07	13.87	15.61	37.65	39.60	19.59	21.82
						SegFormer B5							
Base	VR	72.70	72.67	09.58	11.22	71.27	71.21	19.25	22.15	69.95	69.87	28.38	32.22
	PM	72.24	72.19	09.73	11.32	71.05	71.00	19.32	22.18	69.75	69.64	28.57	32.32
	E	72.93	72.80	09.47	11.01	71.84	71.79	18.83	21.77	70.47	70.46	28.09	32.03
Noise	VR	70.16	70.08	09.29	10.96	69.24	69.22	18.66	21.70	68.26	68.20	27.78	31.80
	PM	69.36	69.36	09.30	10.92	69.00	68.94	18.82	21.81	68.08	68.02	27.87	31.87
	E	71.56	71.48	09.34	10.99	70.72	70.54	18.61	21.78	68.74	68.77	27.30	31.54
	AV	69.60	69.58	08.94	10.26	68.89	68.89	17.37	19.75	68.13	68.16	25.14	28.08
	MV	69.83	69.78	09.03	10.39	68.77	68.92	17.49	20.04	68.30	68.16	25.17	28.07
	B	68.81	68.80	08.88	10.21	67.70	67.64	16.99	19.23	66.81	66.66	24.81	27.69
Scale	VR	**77.93**	**77.94**	10.22	11.91	76.02	76.08	20.21	23.45	74.41	74.45	**30.01**	**34.19**
	PM	75.47	75.56	09.87	11.43	74.68	74.77	20.04	23.06	73.60	73.63	29.95	34.02
	E	75.50	75.60	09.76	11.42	75.39	75.33	19.60	22.63	74.43	74.41	29.45	33.66
	AV.	67.95	68.02	08.96	10.33	68.42	68.45	18.39	21.15	69.37	69.32	28.13	31.94

	MV.	66.71	66.83	08.83	10.13	68.17	68.16	18.40	21.12	69.45	69.33	28.25	31.95
	B	69.76	69.68	09.21	10.68	68.56	68.62	18.32	21.08	68.93	68.88	27.78	31.49
Drop	VR	72.80	72.78	09.66	11.28	71.46	71.37	19.38	22.24	70.06	69.97	28.56	32.37
	PM	72.48	72.43	09.75	11.30	71.25	71.16	19.40	22.19	69.84	69.74	28.59	32.34
	E	72.92	72.78	09.47	10.98	71.92	71.81	18.99	21.88	70.55	70.56	27.98	31.86
	AV	75.17	74.96	09.59	10.93	73.69	73.33	18.39	20.67	72.07	71.87	26.53	29.74
	MV	75.22	74.96	09.58	10.84	73.62	73.33	18.30	20.62	72.26	72.06	26.56	29.70
	B	74.30	73.99	09.48	10.74	72.36	72.05	18.21	20.52	70.46	70.54	26.30	29.47

The results on Dark Zurich suggest much the same things as those on Cityscapes and ADE20K that Scale with simpler metrics is probably the best choice. One major difference is that if domain shift is expected, it is better to use the largest difference thresholding method than a maximum fraction of allowed pixels.

C Calibration Experiments

In order to improve our results we run experiments on calibrated OneFormer ConvNeXt-L and SegFormer B5 models. Specifically, we use temperature scaling on the logits during softmax computation to calibrate the models. We use temperatures of 0.2 and 2 for OneFormer and SegFormer models respectively. We first show the calibration results of such scaling in Table 18. Model calibration is evaluated using Expected Calibration Error (ECE) and Brier Score (BS). As can be seen after temperature scaling both models are better calibrated.

Table 18: Micro and macro-averaged (μ and M, respectively) Expected Calibration Error (ECE) and Brier Score (BS) for OneFormer ConvNeXt-L and SegFormer B5 models on the Cityscapes dataset

Calibration Status	ECE ↓ μ Avg.	ECE ↓ M Avg.	BS ↓ μ Avg.	BS ↓ M Avg.
OneFormer ConvNeXt-L				
Uncalibrated	0.7887	0.8383	0.8012	0.8011
Calibrated	**0.1173**	**0.1084**	**0.0668**	**0.0681**
SegFormer B5				
Uncalibrated	0.0631	0.0160	0.0516	0.0524
Calibrated	**0.0282**	**0.0125**	**0.0506**	**0.0514**

We now show the Area Under the Receiver Operating Characteristics (AUROC) as well as the Area Under the Precision Recall Curve (AUPRC) in Table 19 and Table 20, respectively. We observe that in almost all cases the calibrated models perform better than uncalibrated ones. The only departure from this pattern is AUPRC for SegFormer B5 with the Scale setting.

Table 19: Micro and macro-averaged (μ and M, respectively) Area Under Receiver Operating Characteristic (AUROC) for uncalibrated and calibrated models on the Cityscapes dataset.

Scenario	Uncertainty Metric	Uncalibrated AUROC ↑ μ Avg.	Uncalibrated AUROC ↑ M Avg.	Calibrated AUROC ↑ μ Avg.	Calibrated AUROC ↑ M Avg.
OneFormer ConvNeXt-L					
Base	Var. Ratio	*0.7265*	*0.8822*	**0.8458**	**0.8848**
	Prob. Margin	*0.7893*	**0.9073**	**0.8543**	*0.8913*
	Entropy	*0.7089*	*0.8569*	**0.8387**	**0.8896**

Scale	Var. Ratio	*0.7647*	*0.8972*	**0.8896**	**0.9163**
	Prob. Margin	*0.8305*	*0.9215*	**0.8959**	**0.9221**
	Entropy	*0.7350*	*0.8736*	**0.8805**	**0.9166**
	Avg. Var.	*0.7835*	*0.7880*	**0.8268**	**0.8324**
	Max. Var.	*0.7637*	*0.7677*	**0.8383**	**0.8453**
	BALD	*0.8173*	*0.8213*	**0.8496**	**0.8563**
	SegFormer B5				
Base	Var. Ratio	*0.8830*	*0.9087*	**0.9328**	**0.9468**
	Prob. Margin	*0.8892*	*0.9142*	**0.9351**	**0.9485**
	Entropy	*0.8997*	*0.9234*	**0.9357**	**0.9467**
Scale	Var. Ratio	*0.9212*	*0.9391*	**0.9459**	**0.9569**
	Prob. Margin	*0.9245*	*0.9418*	**0.9477**	**0.9582**
	Entropy	*0.9290*	*0.9459*	**0.9437**	**0.9522**
	Avg. Var.	*0.8678*	*0.8826*	**0.8887**	**0.9010**
	Max. Var.	*0.8687*	*0.8832*	**0.8864**	**0.8978**
	BALD	*0.8947*	**0.9091**	**0.8990**	*0.9067*

Table 20: Micro and macro-averaged (μ and M, respectively) Area Under Precision Recall Curve (AUPRC) for uncalibrated and calibrated models on the Cityscapes dataset.

Scenario	Uncertainty Metric	Uncalibrated				Calibrated			
		AUPRC-Error ↑		AUPRC-Success ↑		AUPRC-Error ↑		AUPRC-Success ↑	
		μ Avg.	M Avg.	μ Avg.	M Avg.	μ Avg.	M Avg.	μ Avg.	M Avg.
	OneFormer ConvNeXt-L								
Base	Var. Ratio	*0.1310*	*0.3090*	*0.9853*	**0.9633**	**0.2834**	**0.3173**	**0.9888**	*0.9611*
	Prob. Margin	*0.2300*	**0.3562**	*0.9885*	**0.9722**	**0.3107**	*0.3397*	**0.9892**	*0.9645*
	Entropy	*0.1193*	*0.2832*	*0.9847*	*0.9548*	**0.2685**	**0.3078**	**0.9885**	**0.9669**
Scale	Var. Ratio	*0.1704*	*0.3258*	*0.9871*	*0.9741*	**0.3169**	**0.3417**	**0.9918**	**0.9786**
	Prob. Margin	*0.2921*	**0.3808**	*0.9905*	*0.9794*	**0.3565**	*0.3717*	**0.9922**	**0.9797**
	Entropy	*0.1424*	*0.2903*	*0.9860*	*0.9702*	**0.2858**	**0.3198**	**0.9922**	**0.9822**
	Avg. Var.	*0.1567*	*0.2303*	*0.9931*	*0.9886*	**0.3136**	**0.2989**	**0.9949**	**0.9917**
	Max. Var.	*0.1391*	*0.2101*	*0.9924*	*0.9883*	**0.3029**	**0.2885**	**0.9951**	**0.9915**
	BALD	*0.1916*	*0.2515*	*0.9928*	*0.9897*	**0.2984**	**0.2959**	**0.9941**	**0.9918**
	SegFormer B5								
Base	Var. Ratio	*0.3873*	*0.4049*	*0.9969*	**0.9963**	**0.3901**	**0.4062**	**0.9975**	*0.9962*
	Prob. Margin	*0.3771*	*0.3935*	*0.9969*	0.9963	**0.3831**	**0.3998**	**0.9976**	0.9963
	Entropy	**0.3840**	**0.4038**	*0.9966*	*0.9961*	*0.3382*	*0.3486*	**0.9975**	**0.9965**
Scale	Var. Ratio	**0.4335**	**0.4422**	*0.9976*	**0.9971**	*0.4204*	*0.4327*	**0.9980**	*0.9968*
	Prob. Margin	**0.4185**	*0.4256*	*0.9976*	**0.9971**	*0.4146*	**0.4258**	**0.9980**	*0.9969*
	Entropy	**0.4099**	**0.4233**	*0.9975*	*0.9965*	*0.3439*	*0.3524*	**0.9977**	**0.9970**
	Avg. Var.	**0.3371**	**0.3334**	**0.9975**	**0.9971**	*0.2716*	*0.2673*	*0.9961*	*0.9954*
	Max. Var.	**0.3352**	**0.3303**	**0.9975**	**0.9971**	*0.2596*	*0.2546*	*0.9960*	*0.9952*
	BALD	**0.3186**	**0.3155**	**0.9960**	**0.9955**	*0.2409*	*0.2391*	*0.9958*	*0.9949*

D Experiments With Noisy Inputs

Here, we provide the results of our experiments with noisy inputs. This experiment was only performed on the Cityscapes dataset with DRN D-22 and OneFormer ConvNeXt-L models. Table 21 shows the base performances across varying noise levels.

As noise levels increase, we see a decrease in performance for both models, although, as seen earlier DRN gives much worse outputs than OneFormer. DRN's calibration also worsens with each noise level, whereas OneFormer's calibration stays mostly the same.

Table 21: Micro and macro-averaged (μ and M, respectively) Mean Intersection Over Union (mIoU), Expected Calibration Error (ECE) and Brier Score (BS) on the Cityscapes dataset for noisy inputs.

Noise Level	mIoU ↑		ECE ↓		BS ↓	
	μ Avg.	M Avg.	μ Avg.	M Avg.	μ Avg.	M Avg.
			DRN D-22			
None	**0.6790**	**0.5479**	0.0380	**0.0177**	**0.0808**	**0.0824**
Std. 5	0.4961	0.4497	0.0897	0.0619	0.1810	0.1828
Std. 10	0.3066	0.2928	**0.0288**	0.1733	0.4327	0.4325
Std. 25	0.1071	0.1034	0.0700	0.3995	0.9390	0.9349
Std. 50	0.0311	0.0312	0.0917	0.5574	1.2908	1.2878
			OneFormer ConvNeXt-L			
None	**0.8287**	**0.6733**	0.7887	0.8383	0.8012	0.8011
Std. 5	0.8149	0.6639	0.7912	0.8365	0.8014	0.8014
Std. 10	0.7979	0.6525	0.7874	0.8325	0.8013	0.8013
Std. 25	0.7413	0.6053	0.7693	0.8176	0.8012	0.8009
Std. 50	0.6202	0.5179	**0.7505**	**0.7770**	**0.7996**	**0.7992**

Table 22 shows the results of using the largest difference as a thresholding technique on noisy inputs and AUROC values. Table 23 shows the results of using a maximum fraction of pixels allowed as thresholding.

As seen with Dark Zurich, the largest thresholding technique becomes better as noise levels increase, with better Precision and Recall. In contrast, a maximum fraction of pixels thresholding works better at lower noise.

Table 22: Micro and macro-averaged (μ and M, respectively) Area Under Receiver Operating Characteristic (AUROC) and Precision, Recall and the fraction of pixels selected for largest difference thresholding on the Cityscapes dataset for noisy inputs.

Noise Level	Uncertainty Metric	AUROC ↑		Largest Difference Thresholding					
				Precision ↑		Recall ↑		Pixel %	
		μ Avg.	M Avg.	μ Avg.	M Avg.	μ Avg.	M Avg.	μ Avg.	M Avg.
				DRN D-22					
None	Var. Ratio	0.9118	0.9277	21.10	20.18	92.13	94.71	23.29	23.51
	Prob. Margin	0.9152	0.9302	19.71	18.84	93.31	95.62	25.26	25.48
	Entropy	**0.9205**	**0.9337**	17.52	16.74	95.04	**96.89**	28.94	29.21
Std. 5	Var. Ratio	0.8413	0.8618	30.23	29.08	84.43	87.70	31.78	31.86
	Prob. Margin	0.8450	0.8650	28.71	27.64	86.27	89.29	34.19	34.27
	Entropy	0.8554	0.8732	26.34	25.36	89.41	91.86	38.63	38.74
Std. 10	Var. Ratio	0.7718	0.7805	43.73	42.55	82.88	84.59	50.24	50.14
	Prob. Margin	0.7735	0.7816	42.39	41.23	85.17	86.68	53.25	53.15
	Entropy	0.7866	0.7934	40.22	39.09	89.29	90.40	58.84	58.75
Std. 25	Var. Ratio	0.6966	0.6857	67.14	66.38	92.13	92.24	80.87	80.71
	Prob. Margin	0.6887	0.6776	66.38	65.63	93.47	93.55	82.98	82.83
	Entropy	0.7156	0.7041	65.11	64.43	**96.37**	96.45	87.23	87.10
Std. 50	Var. Ratio	0.6294	0.6082	**84.63**	**84.46**	95.09	95.14	92.66	92.61
	Prob. Margin	0.6240	0.6027	84.40	84.22	95.88	95.92	93.68	93.64

	Entropy	0.6427	0.6213	83.67	84.06	88.34	89.15	87.06	87.31
				OneFormer ConvNeXt-L					
None	Var. Ratio	0.7265	0.8822	15.02	16.52	84.68	87.75	18.03	18.17
	Prob. Margin	0.7893	0.9073	14.37	15.63	89.19	91.32	19.84	19.98
	Entropy	0.7089	0.8569	14.13	16.23	81.30	84.88	18.40	18.65
Std. 5	Var. Ratio	0.7189	0.8828	15.66	17.20	85.86	88.09	18.59	18.74
	Prob. Margin	0.7846	**0.9082**	14.70	15.91	90.27	**91.91**	20.82	20.98
	Entropy	0.6975	0.8504	14.96	16.88	80.37	84.16	18.23	18.31
Std. 10	Var. Ratio	0.7225	0.8737	15.70	17.35	85.73	87.67	20.51	20.69
	Prob. Margin	**0.7902**	0.9039	15.00	16.13	**90.42**	91.79	22.64	22.83
	Entropy	0.7008	0.8431	15.25	17.26	80.37	83.66	19.79	20.01
Std. 25	Var. Ratio	0.7071	0.8506	16.76	18.45	82.89	85.96	25.13	25.36
	Prob. Margin	0.7771	0.8858	16.01	17.45	88.52	90.84	28.08	28.29
	Entropy	0.6810	0.8173	16.21	18.35	78.04	81.50	24.46	24.61
Std. 50	Var. Ratio	0.6706	0.7929	19.69	21.88	75.11	79.44	33.35	33.54
	Prob. Margin	0.7432	0.8416	**20.11**	21.58	84.53	86.92	36.74	36.94
	Entropy	0.6375	0.7544	19.36	**22.07**	68.96	73.90	31.14	31.33

Table 23: Micro and macro-averaged (μ and M, respectively) Precision and Recall for thresholding based on a maximum fraction of pixels allowed on the Cityscapes dataset for noisy inputs.

Noise Level	Unc. Metric	Max 5% pixels				Max 10% pixels				Max 15% pixels			
		Precision ↑		Recall ↑		Precision ↑		Recall ↑		Precision ↑		Recall ↑	
		μ	M	μ	M	μ	M	μ	M	μ	M	μ	M
						DRN D-22							
None	VR	45.19	45.40	41.52	50.74	35.04	35.18	64.13	73.92	28.48	28.45	76.44	84.64
	PM	44.66	44.83	41.35	50.58	34.77	34.92	64.13	73.95	28.14	28.19	**76.51**	**84.74**
	E	44.04	44.23	39.76	48.74	34.80	35.03	63.64	73.61	28.11	28.23	76.42	84.73
Std. 5	VR	54.97	55.12	23.54	29.69	47.63	47.73	41.16	49.70	42.10	42.13	54.23	63.15
	PM	53.45	53.56	23.09	29.26	47.06	47.17	40.89	49.50	41.71	41.77	54.16	63.14
	E	55.09	55.13	23.23	28.93	48.08	48.25	40.97	49.43	42.23	42.35	54.47	63.39
Std. 10	VR	67.13	67.11	12.20	14.46	62.14	62.10	22.95	26.78	58.77	58.69	32.73	37.61
	PM	63.41	63.41	11.63	13.83	60.68	60.64	22.57	26.38	57.95	57.88	32.44	37.32
	E	68.83	68.73	12.52	14.77	64.07	63.95	23.34	27.10	60.27	60.19	32.97	37.82
Std. 25	VR	81.70	81.65	06.61	06.99	79.06	79.02	12.92	13.61	77.02	76.97	19.09	20.07
	PM	75.67	75.68	06.03	06.37	75.10	75.09	12.37	13.03	74.55	74.52	18.63	19.58
	E	83.90	83.86	06.77	07.16	82.12	82.05	13.40	14.13	80.52	80.45	19.86	20.87
Std. 50	VR	88.49	88.46	05.06	05.11	88.09	88.06	10.24	10.33	87.80	87.76	15.46	15.58
	PM	86.81	86.76	04.82	04.85	86.71	86.65	10.07	10.14	86.63	86.56	15.35	15.46
	E	**89.38**	**89.35**	05.12	05.17	89.02	88.97	10.32	10.40	88.78	88.72	15.56	15.69
						OneFormer ConvNeXt-L							
None	VR	32.16	32.31	47.73	57.40	24.77	24.84	67.92	77.28	20.80	21.03	74.47	82.96
	PM	33.41	33.78	50.18	60.30	24.95	24.99	71.11	80.37	20.58	20.68	79.04	**86.67**
	E	30.89	31.47	44.48	54.09	23.82	24.11	64.18	74.15	20.07	20.51	70.79	79.86
Std. 5	VR	33.39	33.47	46.82	55.89	25.65	25.84	67.10	76.08	21.72	21.79	76.17	83.03
	PM	34.87	35.01	49.54	58.84	26.23	26.34	70.75	79.39	21.61	21.63	**79.90**	86.48
	E	32.06	32.15	43.67	52.72	24.64	24.94	63.04	72.49	20.95	21.27	71.34	79.12
Std. 10	VR	34.62	34.73	44.15	52.27	26.98	27.09	65.58	73.98	22.53	22.66	74.42	81.57
	PM	36.58	36.73	47.19	55.44	27.76	27.82	69.51	77.30	22.83	22.83	79.17	85.34
	E	33.13	33.47	41.06	49.09	25.98	26.28	61.66	70.25	21.70	21.95	70.92	78.15

Std. 25	VR	38.64	38.71	36.11	42.76	31.73	31.80	58.76	66.09	26.75	26.78	69.95	76.44
	PM	41.41	41.45	39.21	46.05	33.05	33.15	62.47	69.61	27.47	27.47	74.83	80.59
	E	36.77	36.65	32.98	39.34	30.38	30.56	54.93	62.39	25.65	25.85	65.64	72.39
Std. 50	VR	47.30	47.37	25.49	31.07	41.07	41.14	44.32	51.89	35.91	35.85	56.27	63.68
	PM	**49.59**	**49.81**	27.03	32.95	43.02	42.94	47.25	54.86	37.62	37.51	61.20	68.13
	E	44.83	44.97	22.80	28.00	39.28	39.36	40.75	48.10	34.38	34.49	51.40	59.02

E Classwise Results

Finally, we provide classwise results for some of the experiments. Table 24 shows classwise Mean Intersection Over Union (mIoU) for all tested networks on the Cityscapes dataset, and Table 25 shows the same for ADE20K dataset. We observe that the best and worst classes in each dataset are consistent across models.

Table 24: Classwise micro and macro averaged (μ and M respectively) Mean Intersection Over Union (mIou) on the Cityscapes dataset across different models. Higher is better. The top five classes for every model are highlighted in bold green, and the worst five classes are highlighted in red italics.

Class	DRN D-22		DRN D-105		OF ConvNeXt-L		OF Swin-L		Segformer B5	
	μ Avg.	M Avg.	μ Avg.	M Avg.	μ Avg.	M Avg.	μ Avg.	M Avg.	μ Avg.	M Avg.
road	**0.9721**	**0.9390**	**0.9815**	**0.9492**	**0.9858**	**0.9553**	**0.9847**	**0.9561**	**0.9847**	**0.9524**
sidewalk	0.7966	0.6962	0.8498	0.7424	0.8775	0.7710	0.8673	0.7646	0.8735	0.7671
building	**0.9019**	**0.8461**	**0.9249**	**0.8744**	**0.9371**	**0.8926**	**0.9401**	**0.8965**	**0.9375**	**0.8947**
wall	*0.3805*	*0.1526*	*0.4826*	*0.2291*	*0.5081*	*0.3053*	*0.6663*	*0.2973*	*0.6960*	*0.3196*
fence	*0.4654*	*0.1716*	*0.5877*	*0.2515*	*0.6937*	*0.2809*	*0.6951*	*0.2886*	*0.6754*	*0.3224*
pole	0.5877	0.5258	0.6632	0.6062	*0.7235*	0.6665	*0.7217*	0.6683	*0.6964*	0.6454
traffic light	0.6301	0.3537	0.7289	0.4734	0.7678	0.5816	0.7644	0.5589	0.7547	0.5632
traffic sign	0.7300	0.6192	0.8053	0.7024	0.8445	0.7566	0.8517	0.7639	0.8231	0.7385
vegetation	**0.9114**	**0.8696**	**0.9261**	**0.8914**	0.9352	**0.9058**	**0.9322**	**0.9006**	**0.9316**	**0.8999**
terrain	0.5697	0.2557	*0.6229*	0.2790	*0.6968*	*0.3332*	*0.6589*	*0.3072*	*0.6684*	*0.3351*
sky	**0.9372**	**0.8121**	**0.9511**	**0.8418**	**0.9573**	**0.8787**	**0.9588**	**0.8719**	**0.9567**	**0.8711**
person	0.7741	0.5214	0.8316	0.6098	0.8743	0.6760	0.8692	0.6546	0.8494	0.6344
rider	*0.5208*	0.3254	0.6300	0.4560	0.7465	0.5362	0.7267	0.5055	*0.6856*	0.4777
car	**0.9234**	**0.8230**	**0.9484**	**0.8794**	**0.9649**	**0.9029**	**0.9642**	**0.8985**	**0.9571**	**0.8971**
truck	*0.4067*	*0.1188*	*0.5999*	*0.2143*	0.9029	*0.3239*	0.9004	*0.3501*	0.8632	*0.3581*
bus	0.6826	0.2365	0.8080	0.4289	**0.9410**	0.5502	0.9299	0.5614	0.9214	0.5964
train	0.5291	*0.0765*	*0.5681*	*0.2004*	0.8790	0.4827	0.8473	0.4778	0.8354	0.3840
motorcycle	*0.4534*	*0.1361*	0.6456	*0.2572*	*0.7136*	*0.2762*	*0.6961*	*0.3006*	0.7412	*0.3570*
bicycle	0.7287	0.4793	0.7918	0.5730	0.7953	0.6099	0.7717	0.5694	0.8022	0.5964

Table 25: Classwise micro and macro averaged (μ and M respectively) Mean Intersection Over Union (mIou) on the ADE20K dataset across different models. Higher is better. The top five classes for every model are highlighted in bold green, and the worst five classes are highlighted in red italics.

Class	OF ConvNeXt-L		OF Swin-L		Segformer B5	
	μ Avg.	M Avg.	μ Avg.	M Avg.	μ Avg.	M Avg.
wall	0.8067	0.6516	0.8145	0.6618	0.7856	0.6381
building	0.8439	0.6402	0.8566	0.6479	0.8214	0.6160
sky	**0.9483**	**0.8759**	**0.9506**	**0.8790**	**0.9453**	**0.8648**
floor	0.8459	0.7415	0.8456	0.7434	0.8220	0.7262

tree	0.7759	0.6058	0.7753	0.6108	0.7477	0.5786
ceiling	0.8583	0.7567	0.8542	0.7483	0.8490	**0.7379**
road	0.8463	0.6934	0.8603	0.7142	0.8580	0.6668
bed	**0.9170**	**0.8345**	**0.9106**	**0.8051**	**0.8991**	**0.7446**
window	0.6355	0.5212	0.6638	0.5158	0.6120	0.4749
grass	0.7153	0.4215	0.7346	0.4164	0.7024	0.3966
cabinet	0.6241	0.3613	0.6379	0.4008	0.6327	0.3527
sidewalk	0.7021	0.5364	0.7059	0.5269	0.6682	0.4679
person	0.8623	0.6387	0.8622	0.6348	0.8258	0.5858
ground	0.3729	0.1986	0.4212	0.2239	0.3781	0.2129
door	0.5428	0.3631	0.5742	0.3691	0.4766	0.3215
table	0.6608	0.4943	0.6908	0.5068	0.6112	0.4095
mountain	0.6218	0.4125	0.6210	0.4709	0.6123	0.4474
plant	0.5788	0.3617	0.5737	0.3593	0.4870	0.3139
curtain	0.7856	0.6775	0.8282	0.7015	0.7346	0.5954
chair	0.6585	0.4655	0.6731	0.4784	0.5906	0.3688
car	0.8771	0.6539	0.8848	0.6554	0.8599	0.5979
water	0.5550	0.3294	0.5965	0.3596	0.5875	0.3113
painting	0.7703	0.6583	0.7710	0.6517	0.7460	0.5801
sofa	0.7240	0.5361	0.7717	0.6058	0.6761	0.4785
shelf	0.4346	0.2814	0.5085	0.2834	0.4334	0.1944
house	0.4782	0.2273	0.4705	0.2188	0.3589	0.2050
sea	0.6542	0.6539	0.6563	0.6657	0.6163	0.6404
mirror	0.7409	0.4859	0.7459	0.5405	0.6822	0.4619
rug	0.6931	0.5074	0.6697	0.5201	0.5712	0.4658
field	0.3654	0.2385	0.3744	0.2600	0.3234	0.2377
armchair	0.4767	0.3774	0.5408	0.4324	0.4380	0.3323
seat	0.6794	0.4377	0.6271	0.3935	0.6062	0.2640
fence	0.4816	0.2270	0.4778	0.2090	0.4450	0.1653
desk	0.5720	0.3196	0.5498	0.3065	0.5174	0.2196
rock	0.6209	0.3134	0.6251	0.3511	0.4836	0.2421
wardrobe	0.4637	0.3900	0.5461	0.3966	0.4957	0.2762
lamp	0.7549	0.5837	0.7439	0.5656	0.6543	0.4512
bathtub	0.7890	0.6519	0.7881	0.7054	0.7722	0.5617
railing	0.4077	0.1737	0.4024	0.1923	0.3233	0.1239
cushion	0.7104	0.6211	0.7144	0.6059	0.5829	0.4591
pedestal	0.3440	0.1316	0.3931	0.1337	0.3005	0.1151
box	0.4007	0.2085	0.3680	0.1998	0.3042	0.1335
column	0.5654	0.2827	0.5452	0.2992	0.3971	0.1823
sign	0.4285	0.3156	0.4494	0.3097	0.3753	0.2077
chest	0.4499	0.3279	0.3611	0.3373	0.4488	0.2941
counter	0.5034	0.2014	0.4112	0.2114	0.2756	0.1485
sand	0.5074	0.4246	0.4304	0.4166	0.3661	0.2842
sink	0.7603	0.6281	0.8013	0.6238	0.7293	0.4948
skyscraper	0.3880	0.4413	0.4748	0.4636	0.6001	0.4912
fireplace	0.7373	0.5610	0.7466	0.5621	0.7959	0.5376
refrigerator	0.8125	0.6262	0.7967	0.6240	0.7766	0.5658
grandstand	0.5877	0.4089	0.4502	0.3187	0.4576	0.2347
path	0.2789	0.1794	0.2696	0.1930	0.2415	0.1313
stairs	0.3472	0.1767	0.3306	0.1939	0.3179	0.1396
runway	0.6795	0.5788	0.7157	0.6200	0.7075	0.4809
case	0.6180	0.2870	0.5921	0.3194	0.4926	0.1707
pool table	**0.9529**	0.7290	**0.9521**	**0.8312**	**0.9378**	**0.7310**
pillow	0.6874	0.5569	0.6626	0.5333	0.5727	0.4080

screen door	0.6210	0.6015	0.7174	0.7501	0.6945	0.4878
stairway	0.3473	0.2017	0.4628	0.1861	0.2846	0.1354
river	0.2326	0.2446	0.1674	0.1943	0.1530	0.1384
bridge	0.7893	0.3932	0.8101	0.4119	0.6948	0.2788
bookcase	0.3632	0.3125	0.3668	0.3179	0.3821	0.2812
blind	0.4365	0.2617	0.5201	0.2866	0.4640	0.2325
coffee table	0.6210	0.4195	0.6698	0.4621	0.5341	0.3168
toilet	0.9087	**0.8842**	0.8984	**0.8076**	0.8761	**0.7845**
flower	0.5273	0.3844	0.5180	0.3990	0.4448	0.3256
book	0.5470	0.2751	0.5712	0.2600	0.4917	0.1820
hill	*0.1413*	*0.0699*	*0.0882*	*0.0782*	*0.0699*	*0.0596*
bench	0.7182	0.2913	0.4896	0.2537	0.4612	0.1472
countertop	0.6699	0.3158	0.6848	0.3225	0.5890	0.3261
stove	0.8335	0.6621	0.8505	0.7050	0.7762	0.5391
palm	0.5766	0.4356	0.5272	0.4224	0.4802	0.3737
kitchen island	0.4398	0.1622	0.3594	0.1433	0.4026	0.2282
computer	0.7565	0.4210	0.7788	0.4522	0.7503	0.3573
swivel chair	0.6038	0.4412	0.5583	0.3940	0.3974	0.3466
boat	0.4278	0.3011	0.6905	0.3579	0.5051	0.2265
bar	0.6650	0.3924	0.5365	0.2896	0.3440	0.2020
arcade machine	0.8454	0.2722	0.6547	0.2077	0.8334	0.2863
hut	0.4318	0.2134	0.3258	0.2070	0.3131	0.1490
bus	**0.9460**	0.3583	**0.9115**	0.2936	**0.9068**	0.2478
towel	0.7651	0.5525	0.7642	0.5077	0.6295	0.3371
light	0.6364	0.4461	0.6482	0.4464	0.5536	0.3497
truck	0.4274	0.1781	0.4698	0.2005	0.4223	0.1556
tower	0.2338	0.1999	0.3230	0.2109	0.1143	0.1274
chandelier	0.7500	0.5696	0.7364	0.5751	0.6495	0.4677
awning	0.4043	0.2681	0.3715	0.2658	0.2873	0.1627
streetlight	0.4746	0.3086	0.4414	0.3132	0.2739	0.1378
booth	0.5275	0.2094	0.6864	0.2372	0.3458	0.2258
television	0.7962	0.6454	0.7413	0.6022	0.7161	0.4806
airplane	0.6213	0.4914	0.6869	0.4720	0.6163	0.3258
dirt track	*0.0322*	*0.0492*	*0.0306*	*0.0237*	*0.0490*	*0.0274*
clothes	0.3764	0.1749	0.4861	0.2240	0.3336	0.1717
pole	0.3596	0.1927	0.3444	0.1895	0.2177	0.1025
land	*0.0627*	*0.0412*	*0.0747*	0.0999	*0.0058*	*0.0056*
bannister	0.2125	0.1589	0.2319	0.1424	0.1263	0.0660
escalator	0.2659	0.3568	0.5813	0.3277	0.5315	0.2616
ottoman	0.4856	0.2862	0.5834	0.3402	0.5115	0.1919
bottle	0.4579	0.2554	0.4654	0.2594	0.3638	0.1409
buffet	0.4452	0.2182	0.4719	0.2150	0.3274	0.1564
poster	0.3500	0.1344	0.2816	0.1522	0.2479	0.0986
stage	0.1463	0.1667	0.1337	0.2894	0.1580	0.1140
van	0.4994	0.1954	0.5293	0.2069	0.4345	0.1864
ship	0.6307	0.3798	0.8245	0.4695	0.7014	0.2476
fountain	0.3263	0.2975	0.4673	0.4499	0.2149	0.1999
conveyer belt	0.7296	0.3313	0.6991	0.2257	0.7720	0.2220
canopy	0.4703	0.2735	0.3512	0.2969	0.4163	0.2003
washing machine	0.7302	0.7117	0.8698	0.7630	0.7532	0.6962
toy	0.4918	0.2208	0.3575	0.2384	0.2614	0.1435
swimming pool	0.8168	0.6303	0.7866	0.4143	0.5739	0.3583
stool	0.5461	0.2621	0.5905	0.2739	0.3919	0.1236
barrel	0.8925	**0.8798**	0.6715	0.5162	0.4894	0.3102

basket	0.3604	0.2936	0.4157	0.3148	0.3615	0.2327
waterfall	0.7514	0.5450	0.5517	0.5178	0.6443	0.3568
tent	**0.9594**	0.4856	**0.9292**	0.5659	**0.9487**	0.3551
bag	0.2520	0.1483	0.2170	0.1410	0.1267	*0.0616*
motorbike	0.7769	0.3167	0.7472	0.3723	0.7456	0.3757
cradle	0.8654	**0.7638**	0.8667	**0.8741**	0.7678	0.7065
oven	0.5860	0.2807	0.5741	0.3720	0.4922	0.2726
ball	0.4123	0.2837	0.5238	0.2504	0.5260	0.1281
food	0.6462	0.2817	0.6334	0.3565	0.3681	0.2434
step	0.1872	0.0850	0.0899	*0.0758*	0.1861	0.0869
tank	0.5648	0.1351	0.5138	0.1449	0.5763	0.1914
trade name	0.3477	0.2577	0.3493	0.2611	0.2678	0.1511
microwave	0.8695	0.6115	0.8657	0.6096	0.7648	0.5329
pot	0.5798	0.3344	0.5933	0.3199	0.4460	0.2539
animal	0.6246	0.4527	0.6330	0.5182	0.5985	0.4072
bicycle	0.6379	0.3518	0.6383	0.3425	0.5816	0.2529
lake	*0.0000*	*0.0000*	0.4752	*0.0994*	0.6027	0.1241
dishwasher	0.7900	0.5149	0.7234	0.4633	0.6610	0.4105
screen	0.6464	0.4130	0.6395	0.4824	0.7059	0.3711
blanket	0.3817	0.3033	0.3442	0.3109	0.1784	0.1382
sculpture	0.6732	0.1532	0.6341	0.1354	0.6072	0.0820
hood	0.6624	0.6031	0.6562	0.6131	0.5749	0.5388
sconce	0.6015	0.3542	0.6167	0.3599	0.4927	0.2539
vase	0.5359	0.3630	0.5246	0.3155	0.4137	0.2371
traffic light	0.4124	0.3142	0.4778	0.2960	0.3619	0.1691
tray	0.1839	0.1243	0.2635	0.1621	0.1173	0.0869
ashcan	0.4290	0.2278	0.4943	0.2422	0.4235	0.1743
fan	0.7102	0.4734	0.7327	0.5408	0.6441	0.3386
pier	0.3749	0.1524	0.3767	0.2290	0.6224	0.1378
crt screen	0.2180	*0.0496*	*0.0694*	*0.0374*	0.1122	*0.0338*
plate	0.6085	0.2960	0.6328	0.2942	0.5125	0.1629
monitor	0.6631	0.2648	0.1195	0.1170	*0.0759*	0.0717
bulletin board	0.6488	0.2437	0.5838	0.1777	0.4835	0.1756
shower	*0.0315*	0.1646	*0.0358*	0.2362	*0.0665*	0.1209
radiator	0.5876	0.3435	0.6938	0.3621	0.6611	0.4215
glass	0.2507	0.1983	0.2497	0.1725	0.1732	0.1312
clock	0.3627	0.3053	0.5175	0.3060	0.4064	0.2080
flag	0.7495	0.4274	0.5406	0.3913	0.5256	0.3048

Table 26 and Table 27 show the Area Under Receiver Operating Characteristic (AUROC) on Cityscapes and ADE20K datasets across a few scenarios. All of the results use entropy as the uncertainty metric. Here also we observe that the best and worst performing classes are generally consistent across different scenarios, especially for Cityscapes.

Table 26: Classwise micro and macro averaged (μ and M respectively) Area Under Receiver Operating Characteristic (AUROC) on the Cityscapes dataset across a couple different models and settings. Higher is better. The top five classes for every model are highlighted in bold green, and the worst five classes are highlighted in red italics.

Class	DRN D-105 Base		DRN D-105 Scale		Segformer B5 Base		Segformer B5 Scale	
	μ Avg.	M Avg.	μ Avg.	M Avg.	μ Avg.	M Avg.	μ Avg.	M Avg.

road	**0.9241**	**0.9783**	**0.9615**	**0.9861**	0.9118	**0.9693**	0.9335	**0.9801**
sidewalk	0.8606	0.8756	0.8996	0.8742	0.8642	0.8826	0.8962	0.8795
building	**0.9235**	**0.9332**	0.9349	**0.9346**	**0.9148**	**0.9293**	0.9280	**0.9353**
wall	*0.6513*	*0.4907*	*0.6980*	*0.4717*	*0.7152*	*0.5491*	*0.7167*	*0.5132*
fence	*0.6946*	0.5896	*0.7400*	0.5685	*0.7387*	*0.6148*	*0.8026*	*0.5933*
pole	*0.7529*	0.7270	0.7550	0.7205	*0.7565*	0.7447	*0.7680*	0.7438
traffic light	0.8339	0.7137	0.8336	0.6879	0.8376	0.7542	0.8491	0.7127
traffic sign	0.8718	0.8388	0.8773	0.8174	0.8523	0.8506	0.8775	0.8292
vegetation	**0.9362**	**0.9366**	**0.9534**	**0.9453**	**0.9286**	**0.9341**	**0.9511**	**0.9484**
terrain	*0.7133*	*0.5592*	*0.7487*	*0.5510*	*0.7117*	*0.5568*	*0.7751*	*0.5526*
sky	**0.9681**	**0.9226**	**0.9708**	**0.9169**	**0.9660**	**0.9223**	**0.9628**	**0.9064**
person	0.9078	0.7937	0.9152	0.7751	0.8952	0.7961	0.9134	0.7807
rider	*0.7214*	0.6861	*0.7483*	0.6808	*0.8223*	0.7011	*0.8396*	0.6993
car	**0.9672**	**0.9422**	**0.9727**	**0.9428**	**0.9464**	**0.9451**	**0.9654**	**0.9495**
truck	0.7554	*0.4891*	0.8498	*0.4899*	0.8737	*0.5390*	**0.9379**	*0.5555*
bus	0.9031	0.7551	**0.9349**	0.7501	**0.9203**	0.7927	**0.9631**	0.7892
train	0.7721	*0.5658*	*0.7414*	*0.5000*	0.8993	0.6744	0.9125	0.6772
motorcycle	0.8312	*0.5072*	0.8179	*0.5009*	0.8516	*0.5942*	0.8607	*0.5732*
bicycle	0.8795	0.7646	0.8984	0.7691	0.8828	0.7628	0.9021	0.7596

Table 27: Classwise micro and macro averaged (μ and M respectively) Area Under Receiver Operating Characteristic (AUROC) on the ADE20K dataset across a couple different models and settings. Higher is better. The top five classes for every model are highlighted in bold green, and the worst five classes are highlighted in red italics.

Class	OF ConvNeXt-L Base		OF ConvNeXt-L Scale		Segformer B5 Base		Segformer B5 Scale	
	μ Avg.	M Avg.	μ Avg.	M Avg.	μ Avg.	M Avg.	μ Avg.	M Avg.
wall	0.5739	0.6680	0.5838	0.6911	0.8406	0.8069	0.8743	0.8182
building	0.5608	0.6452	0.5531	0.6701	0.8300	0.8045	0.8605	0.8039
sky	0.5670	0.7676	0.5786	0.7708	0.9233	**0.9184**	0.9339	**0.9159**
floor	0.5547	0.7259	0.5663	0.7346	0.8556	0.8752	0.8674	0.8720
tree	0.6203	0.7113	0.6428	0.7331	0.8665	0.7693	0.8745	0.7638
ceiling	0.5189	0.7149	0.5099	0.7141	0.8375	0.8589	0.8665	0.8536
road	0.4516	0.7259	0.4608	0.7366	0.8314	0.8193	0.8476	0.8192
bed	0.7180	0.7278	0.6719	0.7245	**0.9456**	**0.9118**	**0.9646**	**0.9123**
window	0.5302	0.6360	0.5263	0.6552	0.7547	0.6916	0.7667	0.6798
grass	0.5200	0.6441	0.5906	0.6610	0.8606	0.7107	0.8761	0.7139
cabinet	0.6989	0.5732	0.7458	0.5806	0.7957	0.5975	0.8219	0.5716
sidewalk	0.5447	0.7314	0.5405	0.7414	0.7642	0.7200	0.8085	0.6995
person	0.6048	0.7202	0.6161	0.7258	0.9108	0.7334	0.9062	0.7070
ground	0.5967	0.4664	0.6169	0.4740	0.6065	0.4299	0.6027	0.4227
door	0.6446	0.6255	0.7004	0.6337	0.6358	0.5255	0.6586	0.4951
table	0.5518	0.6847	0.5349	0.6946	0.7932	0.6604	0.8172	0.6386
mountain	0.7045	0.6829	0.6920	0.7049	0.8066	0.7067	0.8241	0.6949
plant	0.5941	0.5722	0.5973	0.5666	0.7097	0.4936	0.7293	0.4755
curtain	0.5007	0.7722	0.4830	0.7625	0.8088	0.8119	0.8318	0.8035
chair	0.5607	0.6705	0.5258	0.6773	0.6841	0.6138	0.7018	0.5877
car	0.6087	0.8017	0.6218	0.8141	0.9002	0.7805	0.9236	0.7674
water	0.5340	0.4311	0.5104	0.4271	0.7816	0.5628	0.8001	0.5702
painting	0.5304	0.7683	0.5556	0.7635	0.8534	0.7571	0.8708	0.7384
sofa	0.6279	0.6968	0.6681	0.7309	0.8479	0.7624	0.8404	0.7457

shelf	0.6358	0.4825	0.6114	0.4893	0.7001	0.4210	0.7571	0.4163
house	0.4963	0.4237	0.5240	0.4215	0.5942	0.3930	0.5882	0.3653
sea	0.8416	0.7356	**0.8649**	0.7661	0.5105	0.7815	0.6722	0.7845
mirror	0.5035	0.6449	0.4964	0.6652	0.7857	0.6698	0.7806	0.6288
rug	0.4027	0.5136	0.4490	0.5264	0.6194	0.6740	0.6000	0.6428
field	0.6289	0.4627	0.6797	0.4573	0.7246	0.4810	0.7626	0.4843
armchair	0.6309	0.6297	0.6719	0.6332	0.5639	0.5896	0.6109	0.5765
seat	0.5390	0.5249	0.6303	0.5425	0.8414	0.5146	0.8518	0.5117
fence	0.6256	0.4773	0.6257	0.4841	0.7178	0.3680	0.7237	0.3705
desk	0.5602	0.6556	0.6061	0.6902	0.7862	0.6218	0.8023	0.6075
rock	0.6126	0.4923	0.6155	0.5125	0.7262	0.5525	0.7262	0.5262
wardrobe	0.6437	0.5709	0.7209	0.5765	0.7010	0.5167	0.7658	0.5172
lamp	0.7204	0.7042	0.7100	0.7101	0.8199	0.6966	0.8165	0.6669
bathtub	0.6990	0.7776	0.6818	**0.8174**	0.8999	0.8481	0.8828	0.8086
railing	0.6131	0.4368	0.6146	0.4408	0.6652	0.3275	0.6494	0.3161
cushion	0.4820	0.6654	0.4748	0.6584	0.6816	0.7281	0.7192	0.7051
pedestal	0.6809	0.4428	0.6873	0.4416	0.5481	0.3212	0.5147	0.3059
box	0.6084	0.3712	0.5978	0.3630	0.6921	0.2932	0.6581	0.2552
column	*0.3089*	0.4293	0.4210	0.4016	0.6474	0.4266	0.5982	0.3984
sign	0.5225	0.6147	0.5353	0.5977	0.6341	0.3961	0.5934	0.3425
chest	0.4561	0.5929	0.4538	0.6150	0.5828	0.5883	0.6105	0.5485
counter	0.5578	0.3881	0.6440	0.3824	0.6070	0.3743	0.6560	0.3476
sand	0.7243	0.5635	0.7637	0.5650	0.7968	0.5653	0.8045	0.5613
sink	0.5907	0.7345	0.5826	0.7294	0.8554	0.6905	0.8545	0.6610
skyscraper	0.4182	0.6289	0.3830	0.5981	0.6903	0.7200	0.7077	0.7068
fireplace	0.5034	0.7696	0.6717	**0.8441**	0.9120	0.8033	0.9060	0.7539
refrigerator	0.8346	0.7137	0.8122	0.7293	0.8574	0.7904	0.8890	0.7767
grandstand	**0.8782**	0.5326	0.7779	0.4291	0.8273	0.5412	0.8325	0.4975
path	0.4835	0.3132	0.4781	0.3176	0.5924	0.3287	0.5574	0.3038
stairs	0.5280	0.3520	0.5338	0.3616	0.7095	0.3098	0.5954	0.2824
runway	*0.2676*	0.4812	*0.3359*	0.4756	**0.9490**	0.6891	**0.9581**	0.6515
case	0.6746	0.5060	0.7389	0.5134	0.8008	0.6118	0.8432	0.6066
pool table	0.7485	**0.8723**	0.7391	**0.8845**	0.9305	0.8488	**0.9528**	0.8458
pillow	0.5753	0.7081	0.5782	0.7042	0.7406	0.6275	0.7278	0.5904
screen door	0.3675	0.6923	*0.3557*	0.6841	0.6830	0.6751	0.6335	0.6286
stairway	0.3363	0.3674	0.3572	0.3712	0.7469	0.2621	0.7850	0.2590
river	0.4717	0.3615	0.4526	0.3756	0.3881	0.3104	0.3797	0.2734
bridge	0.6281	0.6242	0.7111	0.6332	0.7987	0.6093	0.8159	0.6052
bookcase	0.5989	0.6119	0.5601	0.5919	0.6138	0.5141	0.6564	0.5434
blind	0.7091	0.3400	0.3707	0.3050	0.5208	0.3672	0.4756	0.3452
coffee table	0.5752	0.6190	0.5177	0.6519	0.8910	0.6605	0.8744	0.6495
toilet	0.7409	0.7570	0.7696	0.7848	0.9246	**0.9070**	0.9500	**0.8863**
flower	0.6332	0.5608	0.6670	0.5665	0.6797	0.5289	0.6650	0.4774
book	0.4242	0.5053	0.5302	0.5146	0.7241	0.4159	0.7423	0.3906
hill	0.6818	0.2886	**0.8445**	0.3153	0.3824	0.1686	0.4030	0.1693
bench	0.6265	0.5043	0.6425	0.4843	0.7980	0.3212	0.7693	0.2662
countertop	0.3637	0.5977	0.4136	0.6233	0.7284	0.7519	0.7343	0.7309
stove	0.4978	0.7285	0.6257	0.7418	0.9168	0.7212	0.9310	0.6986
palm	0.6845	0.6145	0.6536	0.6336	0.6720	0.5673	0.7011	0.5387
kitchen island	0.5199	0.4266	0.6521	0.4332	0.7225	0.6503	0.7809	0.6426
computer	0.8235	0.5815	0.8232	0.5919	0.9081	0.7305	0.8766	0.7051
swivel chair	0.5784	0.6860	0.6574	0.7054	0.6079	0.5702	0.6943	0.5242
boat	**0.8885**	0.5479	**0.9060**	0.5646	0.7252	0.4369	0.7538	0.4301
bar	0.6554	0.4605	0.6270	0.4680	0.7454	0.3915	0.7891	0.3932

arcade machine	0.4072	0.5503	0.5758	0.6500	0.8680	0.7148	0.6931	0.6238
hut	0.5054	0.4863	0.4311	0.4959	0.6138	0.3689	0.6393	0.3997
bus	0.3467	0.4428	0.3641	0.4371	**0.9765**	0.3753	**0.9795**	0.3688
towel	0.7283	0.6239	0.7306	0.6176	0.8701	0.6178	0.8842	0.5967
light	0.6130	0.7420	0.6070	0.7311	0.6760	0.4859	0.6491	0.4352
truck	0.5780	0.4361	0.7299	0.4487	0.7291	0.2699	0.5865	0.2357
tower	0.6639	0.2167	0.7170	0.2161	0.3517	0.3008	0.3304	0.2651
chandelier	0.6425	0.7446	0.6891	0.7516	0.7727	0.7477	0.7470	0.7108
awning	0.7975	0.4976	0.7861	0.4995	0.4719	0.3072	0.4494	0.2566
streetlight	0.6850	0.6345	0.6393	0.6176	0.6430	0.2739	0.6165	0.2448
booth	0.3981	0.2835	0.5152	0.2781	0.6733	0.4017	0.8289	0.4596
television	0.4803	0.7019	0.5252	0.6495	0.9151	0.7664	0.9109	0.7065
airplane	0.8537	0.6929	0.8063	0.6951	0.5502	0.6165	0.5442	0.5876
dirt track	0.4029	*0.0504*	0.4449	*0.0566*	*0.2451*	*0.1159*	*0.2267*	*0.1355*
clothes	0.8325	0.4714	0.7844	0.3999	0.8503	0.4640	0.8761	0.4604
pole	0.5662	0.5002	0.6806	0.5169	0.5469	0.2786	0.5646	0.2776
land	0.4633	*0.1282*	0.5031	*0.1432*	*0.1227*	*0.0465*	*0.1449*	*0.0565*
bannister	0.3417	0.3438	0.3737	0.3525	0.4584	0.1728	0.3413	0.1535
escalator	0.6141	0.4464	0.6299	0.3113	0.7641	0.5747	0.6754	0.5215
ottoman	0.6320	0.4822	0.6135	0.4618	0.8452	0.4835	0.8102	0.4721
bottle	0.6183	0.4295	0.5480	0.4040	0.6643	0.2820	0.5900	0.2440
buffet	0.5471	0.3650	*0.3454*	0.3767	0.6931	0.2672	0.7233	0.2774
poster	0.7482	0.3111	0.8322	0.2891	0.6782	0.2700	0.6315	0.2369
stage	0.7343	0.4193	0.7956	0.4082	0.4942	0.4548	0.4788	0.4133
van	0.4960	0.5453	0.5783	0.5172	0.7748	0.3088	0.7363	0.2792
ship	0.7172	0.6277	0.7486	0.6264	**0.9629**	0.5954	0.9360	0.5856
fountain	*0.2365*	0.6323	0.3632	0.6578	0.7300	0.4035	0.6050	0.3776
conveyer belt	0.7016	0.7340	0.7865	0.7000	0.8565	0.6961	0.7608	0.6925
canopy	0.6832	0.5018	0.7821	0.6180	0.7657	0.5034	0.7937	0.4958
washing machine	**0.9583**	**0.9192**	**0.9575**	**0.9109**	0.9189	0.7947	0.9414	0.8013
toy	0.4970	0.4003	0.5326	0.4043	0.5191	0.4129	0.4756	0.3660
swimming pool	0.8311	**0.8127**	0.8263	0.7989	0.8580	0.8935	0.8550	0.8604
stool	0.6112	0.4539	0.6849	0.4576	0.7468	0.3398	0.7656	0.3160
barrel	**0.8543**	**0.8331**	0.8104	0.7544	0.9399	0.7760	0.9281	0.7556
basket	0.6128	0.5168	0.5646	0.5100	0.7601	0.4798	0.6847	0.3967
waterfall	0.6714	0.6821	0.7421	0.7442	0.8017	0.7390	0.8338	0.7768
tent	0.6744	**0.8092**	0.8069	**0.8461**	**0.9881**	**0.9836**	**0.9890**	**0.9885**
bag	0.5270	0.3574	0.5706	0.3445	0.5483	*0.1569*	0.5100	*0.1343*
motorbike	0.7851	0.6201	0.7966	0.6435	0.9041	0.5442	0.8624	0.4961
cradle	0.4388	0.7722	0.5862	0.8150	0.9401	**0.9206**	0.9374	**0.9253**
oven	0.6352	0.4992	0.7394	0.4804	0.6788	0.4870	0.6820	0.4598
ball	0.7694	0.4742	0.7446	0.4316	0.7972	0.2225	0.8621	0.2144
food	0.6721	0.4196	0.6289	0.4441	0.6922	0.4929	0.6790	0.4987
step	0.3730	*0.1241*	0.4539	*0.1345*	0.7090	*0.1597*	0.6085	*0.1420*
tank	0.7262	0.4008	0.3890	0.3767	0.4738	0.3926	0.4686	0.3903
trade name	0.6069	0.4242	0.6257	0.4519	0.3866	0.2330	0.3488	0.2042
microwave	0.6897	0.6949	0.6350	0.6884	0.8810	0.6676	0.9135	0.6587
pot	0.5060	0.5151	0.4797	0.5167	0.7731	0.4351	0.7853	0.3942
animal	0.5093	0.2945	0.4863	0.2946	0.7762	0.5719	0.7497	0.5512
bicycle	0.6692	0.5936	0.7153	0.5852	0.8083	0.3472	0.8002	0.3154
lake	*0.0234*	*0.0002*	*0.0860*	*0.0001*	0.7880	0.1997	0.8605	0.1997
dishwasher	0.6327	0.6098	**0.8802**	0.6309	0.9222	0.6692	0.8628	0.6224
screen	0.8307	0.4992	0.7236	0.5010	0.8256	0.6681	0.7968	0.6055
blanket	0.3294	0.3658	0.3940	0.3488	0.4154	0.2845	0.3097	0.1913

sculpture	0.5847	0.3240	0.5768	0.3206	0.8343	0.2758	0.8373	0.2807
hood	0.5973	0.6423	0.7049	0.6036	0.5808	0.6882	0.5094	0.5935
sconce	0.7347	0.5145	0.7293	0.5030	0.6491	0.4032	0.6226	0.3479
vase	0.6813	0.6166	0.6540	0.5930	0.7775	0.4159	0.7499	0.3745
traffic light	0.5853	0.6974	0.6836	0.6796	0.6773	0.3443	0.6240	0.3111
tray	0.6858	0.3117	0.6344	0.3108	0.5955	0.2606	0.5262	0.2263
ashcan	0.7771	0.4834	0.7593	0.4636	0.8191	0.3523	0.8039	0.3130
fan	0.6371	0.7163	0.6260	0.6670	0.7506	0.5828	0.7302	0.5493
pier	**0.8935**	0.3398	0.8430	0.3722	0.9237	0.4679	0.8972	0.4443
crt screen	0.4179	*0.1100*	0.5170	*0.1263*	*0.3179*	*0.1178*	*0.2905*	*0.1186*
plate	0.6950	0.5008	0.7655	0.4871	0.8537	0.3461	0.8517	0.3406
monitor	0.7184	0.3013	0.7747	0.2437	*0.1745*	0.2068	*0.1027*	0.1705
bulletin board	0.8242	0.4924	0.7822	0.4840	0.8263	0.4846	0.6846	0.4034
shower	*0.3092*	0.4837	0.5107	0.4570	*0.1334*	0.2059	*0.1273*	0.1660
radiator	0.7408	0.5331	0.7187	0.5401	0.8359	0.6907	0.8150	0.6724
glass	0.5036	0.5833	0.5382	0.5610	0.4016	0.2441	0.4431	0.2217
clock	0.4518	0.4883	*0.3102*	0.4624	0.6924	0.3115	0.6216	0.2572
flag	0.5878	0.6707	0.5870	0.6537	0.6334	0.3984	0.5834	0.3099

F Qualitative results on ADE20K

We show a few qualitative results on the ADE20K dataset for a couple of best and worst performing classes in Figure 5 and Figure 6, respectively. The figures show the original image, the class label being looked at, misclassified pixels, entropy, thresholded entropy values (using the largest difference technique), and the detection performance (green areas show correctly identified misclassified pixels, blue areas are false positives and red areas are false negatives). All of these results are from the Base setting of OneFormer ConvNeXt-L model.

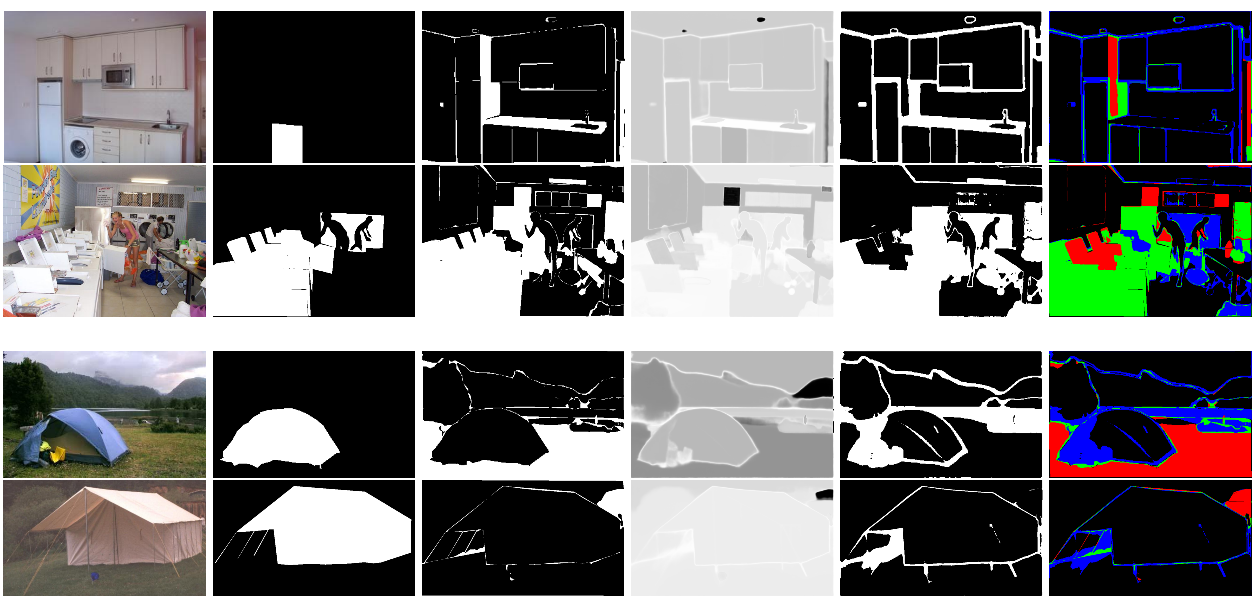

Figure 5: A few images showing a couple of best performing classes in the ADE20K dataset. The first two images include the washing machine class while the last two include the tent class. For each image, we show from left to right, the image, the highlighted class, misclassified pixels, entropy, thresholded entropy, detection mask.

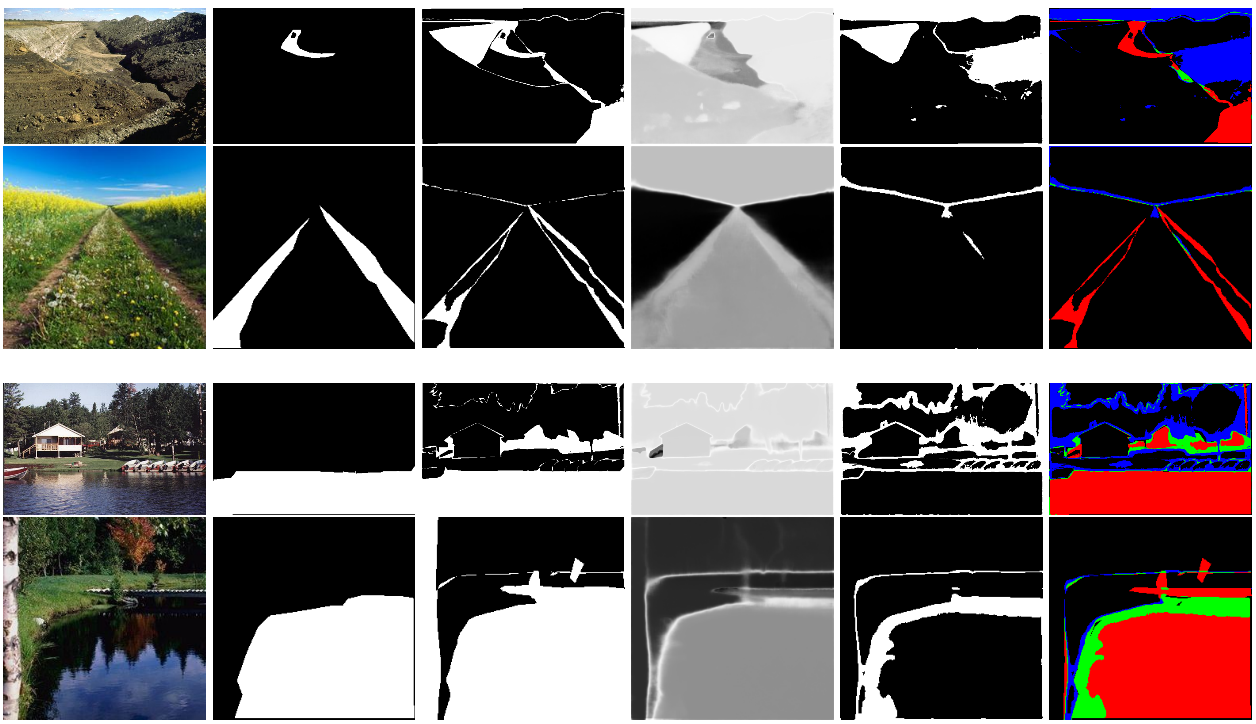

Figure 6: A few images showing a couple of worst performing classes in the ADE20K dataset. The first two images include dirt track class while the last two include the lake class. For each image, we show from left to right, the image, the highlighted class, misclassified pixels, entropy, thresholded entropy, detection mask.